A STUDY OF THE EFFECT OF LAKE ERIE ON DEEP CONVECTIVE SYSTEMS

BY

THOMAS WORKOFF

THESIS

Submitted in partial fulfillment of the requirements
for the degree of Master of Science in Atmospheric Sciences
in the Graduate College of the
University of Illinois at Urbana-Champaign, 2010

Urbana, Illinois

Advisor:

David A. R. Kristovich, Ph.D.

ABSTRACT

This study examines the effect that Lake Erie, and its corresponding marine boundary layer (MBL), have on pre-existing convective storms which propagate over the water surface. To do this, data collected from the 2001-2007 period was analyzed to identify trends in storm behavior over Lake Erie based on season, time of day, convective type and changes in surface-based atmospheric instability due to the lake. Additionally, a study of the 26 July 2005 squall line case was conducted to identify processes by which the squall line interacted with a cool MBL, as well the effects on the convection caused by the movement from land to water.

Results of the climatological study identified 89 cases of pre-existing convection (>45 dBZ) that moved over Lake Erie during the 7-year period. Of these storms, 24 were classified as 'clusters', 20 'isolated', 27 'linear' and 18 'complex.' The evolution of each type of convective system, depicted by changes in the storm's maximum base reflectivity after spending 30 and 60 minutes over the water, was related to environmental parameters characterizing the change in surface conditions over Lake Erie. Analyses revealed that noteworthy changes in the maximum reflectivity of the systems did not occur until 60 minutes over the water. Additionally, cluster and isolated systems tended to weaken in cases where the over-lake environment was convectively unfavorable (i.e. reduced surface-based instability), while linear and complex systems tended to be less affected the lake, regardless of the over-lake conditions. Correlations conducted between several parameters and maximum reflectivity change suggest that no one parameter was the cause of the observed storm behavior over the lake, although linear systems showed high correlation of storm weakening in cases of small low-level (2.5 km) vertical wind shear.

The squall line case of 26 July 2005 was examined in order to understand processes by which Lake Erie and its associated MBL can influence a mature squall line. On this date, a squall line developed over eastern Michigan and propagated eastward over the relatively cool surface of Lake Erie. Surface observations show the presence of a cooler, mesoscale airmass located over and north of Lake Erie (~5^{o}C cooler than the surrounding land). The effect of the MBL on the squall line was hypothesized based on previous squall line theory which relates storm intensity to the ratio between squall line's cold pool intensity and the ambient low-level wind shear.

Results show that the squall line's cold pool would have encountered a MBL which became increasing deep and cooler at the surface as it moved east through southern Ontario toward Lake Erie. This was expected to reduce cold pool strength by reducing the buoyancy gradient at the cold pool's leading edge. Radar observations show the squall line experienced an increase in maximum reflectivity and a decrease in forward speed as it approached Lake Erie, consistent with previous numerical modeling studies of squall line/cool layer interaction and increasing cold pool strength. As the squall line moved eastward over the lake, the convection interacted with a MBL that became increasingly warmer at the surface and more shallow. This, in combination with the storm experiencing a decrease in surface friction upon movement from land to water, was expected to increase the cold pool strength. Consequently, the squall line was observed to develop two small-scale bow echoes, the convective updraft became tilted toward the rear, and the system experienced an increase in forward speed while over the water. This behavior is agreement with theory regarding the cold pool overwhelming the ambient shear and accelerating forward at the surface. Furthermore, the observed rapid alteration of the system in

correlation with movement from land to water suggests the decrease in friction played a larger role in system alteration than surface-based buoyancy changes.

To my mother and father.
May the story that unfolds in these pages make you proud.

ACKNOWLEDGMENTS

This research was funded National Science Foundation grant ATM 07-11033 and UCAR COMET grant S09-71437.

While it is my name that graces the cover of this Thesis, this project is the summation of the thoughts, ideas and vision of many people, of whom I owe many thanks. First and foremost, I must express my deepest gratitude to my advisor, Dr. David Kristovich, for being such a willing and patient teacher throughout the course of this project. Your insight, knowledge, and guidance have meant the world to me for the past four years. I must thank you for having patience in dealing with my many missteps, typos, and apparent inability to write in the proper verb tense. This project simply would not have been possible without you. Thank you.

Many thanks also to the National Weather Service office in Cleveland, OH, in particular Mr. Robert LaPlante, for providing archived numerical model data that was vital to the 26 July 2005 case, as well as insight that was vital to the climatological study. Thank you to Dr. Neil Laird at Hobart and William Smith Colleges, for many helpful discussions, as well as providing the groundwork methodology used for the climatological portion of this study. Thanks to Dr. Robert Rauber at the University of Illinois, whose sharing of knowledge and insight on squall line theory was in many ways the birthplace for the ideas put forth in the case study. My appreciation also goes out to the members of the Mesoscale/Boundary Layer Research Group at the Illinois State Water Survey, past and present, for their assistance and willingness to lend a helping hand.

Additionally, I would like to thank countless friends and family members who provided love and support throughout this process. Thanks to Joe Clark, Justin Hampton and Andy

VanLoocke, who listened to countless rambling throughout this process, and in many instances, provided helpful suggestions to keep it moving forward. To Hilary Minor, who never let me doubt my ability to answer the questions I asked. Thank you.

Finally, to my mother. Your love and support are the reason I was in position to do this research in the first place. Words will never be able to express how much I respect you and look up to you. Thank you for all that you've ever done.

TABLE OF CONTENTS

Chapter 1
Introduction and Background

1.1 Justification

The Great Lakes (GL) region of North America is home to more than 30 million people (Environmental Protection Agency, http://epa.gov/greatlakes); the weather experienced by many in this region is directly affected by the lakes. The influences of the lakes are most pronounced in areas frequently downwind (i.e. major cities such as Cleveland, OH and Buffalo, NY) since weather systems are often modified by the lakes prior to arriving (Scott and Huff 1996). While much research has been conducted on the mesoscale modification of the atmosphere during cold-season months, much less is known about how the relatively cool lakes affect pre-existing deep convective systems in the warm season. This results in a large degree of uncertainty as to how the structure and severity of storms will be altered as they propagate over the lakes.

Past studies on the climatological locations of deep convective development and movement in North America have shown that the GL region is an active area for organized mesoscale convective systems (Laing and Fritsch 1997, Augustine and Howard 1991). In addition, Johns and Hirt (1987) showed that the GL region is also an area of high derecho activity, meaning not only does the area experience frequent deep convection, but convection that produces severe weather (their Figure 2).

Other previous research (Augustine et al. 1994, Scott and Huff 1996) has found that on climatic time scales the GL suppress clouds and precipitation close to the coastlines during the summer season, particularly regions south and east of the lakes. However, this suppression is a seasonal trend and may not apply to individual storms. This limitation was highlighted by Graham et al. (2004), who showed that mesoscale convective systems (MCS) responded

temperature, suggesting that continued surface-based buoyancy is not always critical to MCS life cycles. While the Graham et al. (2004) study provides important information on the behavior of storms interacting with a cooler lake, it considers only MCS in general, and does not address critical issues such as the physical processes in the storm which may be altered by its interaction with a marine boundary layer (MBL).

The goal of this project is to better understand how interaction with large lakes can modify overlying convection. To achieve this, the study was conducted in two parts: 1) development of a seven-year climatology of convective interaction with Lake Erie, and 2) a detailed analysis of a case study. The climatological study used radar and surface observations from 2001-2007 to identify general convective behavior when interacting with Lake Erie. The case study focuses on 26 July 2005, when a severe squall line developed in Lower Michigan and propagated eastward, eventually moving over the cooler surface of Lake Erie (Figure 1a). While over the lake, the convective system experienced changes in its kinematics and structure, and produced severe surface winds both east and west of the lake (Figure 1b), including a 100 kt wind gust reported by a ship on Lake Erie (personal communication, NWSFO Cleveland, OH, 2007).

1.2 Review of Squall Line Theory

One aspect of this study investigates processes by which the GL can modify pre-existing convection through examination of a squall line event. Modification of squall lines by a lake is a reasonable place to start such an investigation since the structure and life cycle of linear convective systems have been well studied both observationally (i.e. Ogura and Liou 1980, Smull and Houze 1985 and 1987) and through the use of numerical modeling techniques (i.e.

Thorpe et al. 1982, Lafore and Moncrieff 1989, Coniglio and Stensrud 2001). Theoretical concepts developed by these studies are commonly used in operational forecasting of squall lines. The 26 July 2005 case was chosen for this investigation largely because it represents a difficult forecast problem (Robert LaPlante, personal communication, 2006) and the convection underwent significant changes in structure over the lake while continuing to produce severe weather.

Squall lines are self-sustaining linear mesoscale convective systems that tend to develop in environments of small directional wind shear; they propagate as new convective cells develop as environmental air is lifted along the forward edge of the storm's evaporatively-cooled cold pool. At maturity, they feature convection at the leading edge of the cold pool, can have front-to-rear flow at upper levels, and often have been observed to have rear-to-front flow in the mid-levels (referred to as the rear-inflow-jet, RIJ) which can descend to the surface (i.e. Smull and Houze 1987, Weisman 1992, Klimowski 1994).

Weisman et al. (1988) and Rotunno et al. (1988, hereafter RKW) used idealized numerical modeling studies to advance a commonly-cited theory that argues the intensity and structure of squall lines is in part controlled by the circulation (im)balance of horizontal vorticity generated by the storm's cold pool and the ambient environmental low-level vertical wind shear (in their case, they utilized surface-2.5 km shear). 'RKW Theory' describes the interactions of the cold pool and ambient environment through this relative balance of horizontal vorticity. At the early stage of the squall line life-cycle the positive vorticity imported by the ambient low-level shear dominates the system, tilting the updraft in a downshear (relative to the ambient shear) direction (Figure 2a). As the temperature in the cold pool decreases through evaporative processes and the horizontal buoyancy gradient at its forward edge increases, its negative

vorticity generation can eventually equal that of the ambient wind shear, leading to an erect updraft (Figure 2b). RKW refer to this as the 'optimal condition.' With continued cooling of the cold pool, its negative vorticity becomes greater than the environmental positive vorticity importation, allowing the cold pool to dominate and tilt the system in an upshear direction (Figure 2c).

A consequence of 'RKW Theory' is that the squall line is potentially sensitive to factors which change the vorticity generation of the cold pool and ambient environment. The introduction of a lake surface and its associated heat exchanges with the atmosphere would be expected to change both environmental and cold pool characteristics. Changes in the balance of vorticity generation between the cold pool and environment due to variations in surface temperature were illustrated in a numerical model study by Lericos et al. (2007, hereafter L07). L07 focused on squall lines moving eastward from the Gulf of Mexico onto a warmer/cooler land surface along the northern Florida coast, and found that land-breeze circulations (in cases of moderate and strong shear) reduced the amount of ambient wind shear near the shoreline and over land. This decreased the amount of environmental vorticity generation, causing the squall line's updraft to tilt upshear and weaken.

Additionally, Parker (2008) used an idealized numerical model to simulate squall line interactions with low-level cooling. In his study a surface isothermal cool layer, approximately 1 km deep, was introduced to a mature squall line and cooled to four thresholds: -10 K and -12 K (relative to the ambient environment), the temperature deficit of the cold pool at squall line maturity (-14 K), and infinitely. The results showed that until the cool layer becomes approximately 10 K (or greater) cooler than the ambient environment, little change in the squall was observed, suggesting that cold pool forcing can overcome a significant amount of convective

inhibition (CIN) if some convective available potential energy (CAPE) still exits. Furthermore, the study showed a secondary maximum of squall line updraft speed, along with system slowing, as the cool layer is cooled to the temperature of the cold pool. This suggests that the decreasing temperature deficit reduces cold pool strength, bringing it closer to circulation balance with the vertical wind shear, in agreement with RKW Theory principles. In cases where the surface cool layer reached the temperature of the cold pool, the simulated squall line underwent a transition to an elevated system that was driven by bore propagation at the top of the cool layer.

While the conclusions of L07 and Parker (2008) are greatly beneficial in understanding the effect that changing surface features have on squall lines, it is likely that the land breezes studied by L07 and the cool layer used by Parker (2008) are structurally different than offshore flows examined in the present case. The more limited scale of the Great Lakes would be expected to make the MBL more strongly dependent on the prevailing synoptic conditions, meaning a Great Lakes MBL can be highly variable, unlike the symmetric stable layer that developed in L07 or isothermal layer in Parker (2008). This variability in MBL formation and structure would be expected to introduce large variations in buoyancy and wind profiles (and consequently vorticity generation) of the ambient environment with which the squall line interacts.

Additionally, as the cold pool moves from land to water, it would be expected to experience a reduced amount of frictional mixing near the surface. Fankhouser et al. (1992) concluded that frictional mixing must be accounted for when considering the vorticity generation of the cold pool, as frictional mixing is thought to reduce the amount of vorticity produced. The reduction of surface friction associated with movement from land to water would also be expected to affect the squall line by altering the cold pool strength.

One goal of this part of the Thesis research is to diagnose the effect of Lake Erie and its associated MBL on the squall line case of 26 July 2005. To do this, the MBL that existed on that date is characterized, and alteration of cold pool vorticity generation through changing buoyancy gradients and frictional differences is considered. Additionally, MBL-induced changes in surface-based instability on the squall line's intensity, as well as the water surface's effect on system speed, are investigated.

1.3 Review of Marine Boundary Layers

Previous research on MBLs near shorelines has shown that their structure is largely controlled by synoptic environmental conditions and land/water temperature differences. Arritt (1993) found that near coastlines and relatively cool water surfaces, MBLs can range from stable internal boundary layers (IBL), purely advection of warm air over a cooler surface with no corresponding surface-based circulations, to full lake-breeze (sea-breeze) circulations (LBC), or a combination of the two. The varying structure and potential mesoscale circulations of MBLs creates a diversity as to how the MBL can alter the temperature and wind profiles of the atmosphere relative to the convective boundary layer (CBL) over land areas. The magnitude of these variations can potentially affect convective systems, which often depend on the instability and vertical wind shear of the lower atmosphere.

The depth, temperature and wind profiles of the MBL vary greatly depending on whether the MBL is an IBL or has a LBC. An IBL is pure advection of warm air over a cooler surface, with no organized mesoscale circulations. LBCs are mesoscale circulations which alter the low-level wind profile of the atmosphere, a characteristic that has not been conclusively observed with the presence of an IBL. Also, while both LBCs and IBLs are cooler than the CBL over

land, the LBC is well-mixed and tends to be much deeper (~1-2.5 km), compared to an IBL which can be strongly stable and relatively shallow (~100-200 m). The differences in how the two types of MBLs alter the atmosphere can have a large effect on convection, which can be vulnerable to changes in surface based instability and low-level wind shear.

1.3.1 Review of Lake Breeze Circulations

LBCs are mesoscale circulations that form near/over coastlines in response to differential heating between the relatively warm land and cool water surfaces. While LBCs are common in the GL region during the warm season, they are not always observed (i.e. Laird et al. 2001). Biggs and Graves (1962) and Lyons (1972) originally proposed a 'lake-breeze index', ε, to forecast the occurrence of lake breezes on the western shores of Lakes Erie and Michigan. ε is defined as:

$$\varepsilon = \frac{U}{C_p(\Delta T)_{\max}}, \qquad (1)$$

where U is the shore-perpendicular wind (Laird et al. 2001) at an inland surface station, ΔT_{max} is the maximum temperature difference between an inland station and the water surface temperature, and C_p is the specific heat of dry air at a constant pressure (1.003 J K^{-1} g^{-1}). Biggs and Graves (1962) and Lyons (1972) concluded that lake breeze development would be expected when ε <3.0. As can be seen in equation (1), the formation of a LBC is sensitive to the synoptic wind speed (U). This was confirmed in the findings of Laird et al. (2001), who in a 15-year climatology of lake breeze occurrences around Lake Michigan found that ~95% of observed lake breezes occur when the inland surface winds were <5 m s^{-1}.

The presence of LBCs has been identified in previous studies through a wide range of observational platforms. The presence of radar 'fine lines', satellite observations of cloud

formation, as well as abrupt changes in temperature or shifts in wind direction measured by surface observation platforms have all been used to indentify the presence of a LBC (i.e. Wakimoto and Atkins 1994, Laird et al. 2001).

1.3.2 Review of Stable Internal Boundary Layers

In instances of warm air advection over a cooler water surface and an absence of a LBC, previous observational (i.e. Smedman et al. 1997b) and numerical modeling studies (Smedman et al. 1997a, Skyllingstad et al. 2005) have shown evidence of a stable IBL forming near the surface (Figure 3). Angevine et al. (2006) found, using observations taken over the Gulf of Maine, that the IBL was well developed by 10 km offshore. Similarly, in numerical model simulations by Smedman et al. (1997a), a strong stratification zone formed immediately along the coastline (Figure 4). Smedman et al. (1997a) also suggested that the temperature profile of the IBL is highly variable in space and time. Analyses shown in Figure 5 suggest that the IBL is highly stable near the coast, but becomes statically neutral at large fetches and is joined to the boundary layer above by a sharp inversion (Figure 3).

The variable nature of the temperature profile in the IBL makes prediction of its structure difficult. Smedman et al. (1997a) derived the IBL stability parameter ***S,*** which can be used to identify if the IBL is expected to be statically stable or neutral. ***S*** is defined as:

$$S = t^{1/2} f^{1/2} \left(\frac{\Delta\theta}{\theta} \right)^{-1}, \quad t = \frac{X}{V_g} \qquad (2)$$

where **f** is the Coriolis parameter (1.04×10^{-5} at 41^{o}N), $\mathbf{\Delta\theta}$ is the potential temperature difference between land and water, $\mathbf{\theta}$ is a reference temperature (K), **t** is time (s), **X** is over-water fetch (m) and $\mathbf{V_g}$ is the geostrophic wind speed (m s^{-1}). In instances where $\boldsymbol{S}<75$, they considered the IBL statically stable (dotted black line over lake in Figure 3), and when $\boldsymbol{S}>75$ the IBL was considered

statically neutral (solid black line over lake in Figure 3). Skyllingstad et al. (2005) showed that the depth of the newly-formed IBL was related to wind speed, roughness length, heat flux and water temperature. A formula for estimating the depth (T_I) of the IBL[1] was presented in Mulhearn (1981) and Garratt (1990):

$$T_I \approx 0.02U\left(\frac{g(\theta_v - \theta_{vs})}{\theta_v}\right)^{\frac{-1}{2}} x^{\frac{1}{2}} \qquad (3)$$

where **g** is gravity, $\boldsymbol{\theta_v}$ and **U** are the atmospheric virtual potential temperature (K) and wind speed (m s^{-1}) of the mixed layer flowing out over water, $\boldsymbol{\theta_{vs}}$ is the virtual potential temperature of the air immediately above the lake surface and **x** is the overwater fetch (m).

This study examines how the presence of a cool water surface, and associated MBL, associated with a large lake effects pre-existing convection. The climatology portion is used to identify statistical relationships between the atmospheric changes associated with the MBL and changes in convective intensity, while the case study focuses on how the physics of a MBL and changes in surface friction due to the water surface can affect the structure and intensity of a severe squall line. Taken together, these studies aim to increase the understanding of the potential influence cool water surfaces have on the intensity and kinematics of convective storms.

[1] This equation is adapted from Angevine et al. (2006).

Chapter 2
Data and Methodology

2.1 Climatology

A climatological analysis of storm evolution over Lake Erie was developed to identify how different convective types are affected by interaction with the lake's MBL. The study utilized data from 2001-2007 in order to further understanding of how lake-induced changes in the boundary layer, most importantly surface-based stability and wind profiles, affect pre-existing convection crossing the lake. Statistical characteristics of convection/lake interaction were analyzed by season, time of day, convective type and storm behavior to identify common storm responses and the potential causes. The climatology was developed with a focus on the eastern shore of Lake Erie, an area that is frequently downwind of convection crossing a large lake (Laing and Fritsch 1997).

Data from the Cleveland, OH (KCLE) WSR-88D radar (Figure 6) was used for the climatological study. The area of study was chosen to be south of 42.25^{o}N latitude; this was selected to include storms within a range of ~100 km of the radar.

2.1.1 Determination of Cases

2.1.1.1 Identification of Cases via Precipitation Data

Radar data from KCLE for days where convection crossed Lake Erie was constructed to examine storm behavior over the water. However, analyzing all Level II data for the entire 2001-2007 time period, recorded approximately every 5 minutes at KCLE, proved to be an inefficient way to determine instances of convection/lake interaction due to the large time requirements for analyzing such high-resolution data.

A preliminary set of days that may have included pre-existing convection moving over Lake Erie was constructed using daily precipitation data from the Nation Climatic Data Center (NCDC). The precipitation data were examined in the following manner:

1. Only stations that were located 'upwind' of Cleveland, OH were used. 'Upwind' was defined as the range in wind direction from 130-340^{o} which includes 80% of the daily averaged synoptic wind at KCLE over the 2001-2007 time period.

2. Only stations with precipitation data recorded for 90% of the 2001-2007 time period were used. This revealed ten stations (numbered 1-10 on Figure 6, Appendix A).

3. From these ten stations, days on which ≥.5" of precipitation was recorded at at least one site were identified.

4. Since daily precipitation totals are determined as the sum of precipitation collected in the 24-hour period from 0000-2359 LST, it is possible to miss events in which convection occurred during the overnight hours and had ≥.5" of precipitation split between two consecutive days. To avoid missing these cases, an analysis was done to identify dates in which ≥0.5" of rain fell during the overnight period. For U.S. sites, at which precipitation is observed hourly, events were recorded for when ≥0.5" of rain fell between 2100-0300 LST. Since Canadian sites only report daily precipitation amounts, consecutive days in which the sum of total precipitation was ≥0.5" were also added to the list of days that may be appropriate for this study.

5. Any instances that included snow in the precipitation type, or the mean temperature was <0^{o}C, were eliminated.

This analysis identified 387 dates in which the above criteria were met for at least one surface precipitation observation station.

2.1.1.2 *Refinement of Dataset through Radar Data*

To further specify cases of convection/lake interaction, the 387 dates that were identified using precipitation data were then analyzed using composite radar reflectivity imagery (http://www.mmm.ucar.edu/imagearchive/) created by the Mesoscale and Micrometeorology Division of the National Center for Atmospheric Research (NCAR). This was done to eliminate dates when precipitation occurred, but were not likely due to deep convection. Since Lake Erie is not completely visible in any of the regional composites at the NCAR website, national image composites were used. While the national composite lacks the desired resolution, it does allow for cases that are clearly not convective to be identified.

Any date that had a maximum base reflectivity <35 dBZ on the national composite was designated as 'not convective' and eliminated. The 35 dBZ threshold is subjective, but was chosen to ensure no convective events (>45 dBZ) were lost due to the poor resolution of the composite imagery. All other cases were identified as 'potentially convective' and kept for further analysis with Level II radar data. This reduced the dataset to 233 possible dates. It should be noted that one individual date may have included multiple convective cases.

Level II radar data for KCLE was gathered from the NCDC for the approximate times of convective interaction with the lake. Each case was examined with GR2Analyst software (Gibson Ridge, Version 1.60) to determine if pre-existing convection was present and moved across Lake Erie. In order for the case to qualify for this study by having pre-existing convection, base reflectivity ($.5^{o}$ tilt) >45 dBZ, a common threshold for convective rainfall (Robert LaPlante, personal communication, 2007) needed to be present for at least three scans prior to moving over the lake surface. A color-table for base reflectivity was created in

GR2Analyst so that only >45 dBZ reflectivity values were displayed. All cases not meeting the reflectivity criteria were eliminated from the dataset.

In some instances, areas of >45 dBZ reflectivity were imbedded in areas of widespread, heavy rainfall associated with synoptic disturbances such as cyclones. These cases were designated 'synoptic convection/heavy rainfall' events. Since the focus of this climatological analysis is to understand how individual convective systems are affected by passage over Lake Erie, these cases were eliminated from the database. Cases where there were missing Level II radar data or where the convection crossed the lakeshore north of the 42.25^{o}N boundary were also eliminated. This left the database with 89 total cases (Appendix B).

2.1.2 Analysis Parameters of Environmental Conditions

In order to understand the impact Lake Erie has on the convective systems identified for this study, observations of the atmospheric conditions both over land and over water were collected and analyzed. From these data, parameters were created to help characterize changes in the atmosphere induced by the water surface, and identify which lake-induced changes have the greatest effect on convection.

For each case, observations of temperature, wind speed and wind direction were collected from surface observation sites over land on both the upwind and downwind side (relative to storm motion) of Lake Erie. Both the upwind and downwind observation sites used in each case were the sites deemed closest to the path of the convection as determined from radar data. For the upwind site, data were gathered for the time period of four hours before (-4) the storm moved over the water to two hours after (+2) it moved over the water. For the downwind sites, data

were gathered for the time period consisting of two hours before (-2) the storm moved over the water to five hours after (+5) it moved over the water.

Air and water temperature data from National Oceanic Atmospheric Administration (NOAA) buoy 45005 (Figure 6) were gathered for each case for which the buoy was operational (generally April through November). Buoy data were gathered for four hours before (-4) the convection crossed the coastline to four hours after (+4). Rawinsonde observation (RAOB) data were also collected from Detroit, MI (KDTX) and Buffalo, NY (KBUF) to determine surface-2.5 km and surface-6 km wind shear (refer to Figure 6 for RAOB locations). All surface, buoy and RAOB data were acquired via the NCDC, and all soundings were analyzed using the RAOB software program (Environmental Research Services LLC, Version 5.9).

In order to analyze the potential effect Lake Erie and its associated MBL had on the convection, 29 analysis parameters were created from the surface, radar and RAOB data. These parameters were created to characterize changes in atmospheric stability and vertical wind shear around and over the lakes. These parameters and their associated definitions are displayed in Appendix C**.**

2.1.3 Organization of Events by Convective Type

Each convective event in the database was classified according to convective type (Appendix B) in order to identify potential differences in storm behavior due to different storm structures. In instances which convection was observed to change from one type to another over the lake, it was classified as by its observed type as it moved over the water surface. The four types of convection were defined as:

Cluster (CL): Areas of unorganized convection, with several (3 or more) reflectivity maxima located closely together. In order to classify the case as a 'cluster', reflectivity maxima must have been no further apart than 2 diameters of the 45 dBZ reflectivity area of each individual storm. Areas of >45 dBZ reflectivity were generally small in areal coverage (> 40 km^2) for individual storms and were separated by reflectivities <35dBZ.

Isolated (I): Individual convective storms, including supercells. Convection must be separated from other reflectivity maxima by greater than 2 diameters of the >45 dBZ reflectivity area to be included in this category.

Linear (L): The area >45 dBZ reflectivities organized in a linear manner. Storms were considered linear if they were organized in a line <50 km wide and >45 dBZ areas of reflectivity were separated by <20 km and reflectivities >35 dBZ.

Complex (C): Area of >500 km^2 of continuous >45 dBZ reflectivities.

2.1.4 Analyzing Storm Behavior

Level II WSR-88D data from KCLE for each convective case was analyzed using GR2Analyst. The maximum base reflectivity (0.5^o tilt) was recorded for each volume scan beginning at 30 minutes before (-30 mins) the time the convection moved over the water (TMOW). In cases where the convection had not developed at -30 minutes, the maximum reflectivity was recorded beginning at the time when the maximum reflectivity exceeded 35 dBZ. If a reflectivity value of >35 dBZ was not observed at least 15 minutes before the storm crossed the coastline, the case was rejected.

The maximum reflectivity for each case was recorded at each volume scan (approximately every 5 minutes) until the maximum reflectivity fell below 45 dBZ, in which it was declared 'dead', or when the convection moved over land on the downwind shore. In these cases, the maximum reflectivity was recorded for two radar scans after dying or moving over land.

Storm behavior (maximum reflectivity change relative to the maximum reflectivity at the time the convection moved over water, TMOW) was separated into six categories to characterize storm intensity change over the water. These categories were defined as:

Significant Strengthening: ≥ +8 dBZ maximum reflectivity change

Moderate Strengthening: +3 to +7 dBZ maximum reflectivity change

No Change: -2 to +2 dBZ maximum reflectivity change

Moderate Weakening: -3 to -7 dBZ maximum reflectivity change

Significant Weakening: ≥ -8 dBZ maximum reflectivity change

Died: maximum reflectivity falls below 45 dBZ

Storm behavior was determined at four times relative to TMOW: 30 minutes before (-30 mins), 30 minutes after (+30 mins), 60 minutes after (+60 mins) and 90 minutes after (+90 mins). Cases where the convection moved over the downwind shore or died before it could be over the water for 30, 60 or 90 minutes were not assigned associated values.

2.2 Case Study of 26 July 2005

The evolving structure, intensity and associated circulations of the squall line in this case study were examined using Level II WSR-88D radar data from Detroit, MI (KDTX), and Cleveland, OH (KCLE, Figure 6). Since KCLE was closer to the squall line as it moved across

Lake Erie, it provided the highest resolution radar data and was therefore used for most radar analyses in this study. Base reflectivity fields (for the .5^{o} elevation angle) were analyzed to determine convective intensity, location and changes in horizontal structure.

Storm relative velocity (SRV) fields were calculated to determine the circulation patterns within the squall line and identify changes in the flow field that occurred while over the lake. SRV was calculated using average storm-motion, determined from the locations of the leading edge of the squall line (defined as the forward edge of 20 dBZ reflectivity, as in Parker and Johnson 2000) at five latitudes. Average motion based on other commonly-used features (i.e., location of highest reflectivity, approximate center of highest reflectivity) gave storm motions that were often unrealistic. Storm motion was determined for each radar scan (for KCLE, every 5 minutes), while the storm was approaching/travelling over Lake Erie. Cross-sections of SRV were used to monitor the vertical structure of flow fields within the squall line while it moved over the lake.

In order to interpret the factors controlling the storm structure and movement as the squall line moved from land to over Lake Erie, environmental conditions over the land and lake were required. Surface observation sites in the region provide important information on the mesoscale surface variations induced by the lakes. Hourly surface observations from sites near the immediate shore of Lake Erie, as well as inland (blue diamonds on Figure 6, Appendix A), along with data from NOAA buoys 45005 and 45132 on the lake were used to determine surface air and water temperatures, dew point, and wind data on 26 July 2005. Surface observation sites were chosen to give the best coverage and resolution of data upwind, over, and downwind of Lake Erie. Surface and buoy data were obtained from the NCDC.

Observations of atmospheric conditions above the surface in this area are more limited both spatially and temporally than surface observations. RAOB soundings (generated with the RAOB program), taken at 0000 and 1200 UTC at Buffalo, NY (KBUF), Detroit, Michigan (KDTX) and Wilmington, OH (KILN) were used to estimate the surface-based instability and vertical structure of the atmosphere, particularly the calculation of low-level wind shear. Additional information was obtained from velocity-azimuth display (VAD) profiles (radar-derived winds) from Level III WSR-88D radar data from KDTX, KCLE and KBUF to give additional estimates of shear values. Since low-level vertical shear has been identified as an important parameter in squall line intensity and structure (i.e., Weisman and Klemp 1986, RKW), 0-2.5 km wind shear of the component normal to the convective line (east, or U-component, called 2.5 km U-wind shear here) was tabulated for locations nearest the convective path. As can be noted from Figure 6, there were very little observational data over Lake Erie, meaning the vertical structure of the MBL and how it evolved over the lake is largely unresolved from observations.

Archived output of the 00 and 06 hour forecasts of the 1200 UTC initialization of the Global Forecast System, 40 km grid (GFS40) numerical model were used to analyze the synoptic environment and atmospheric stability in the region throughout the afternoon. The model's 40-km resolution appears to be adequate for horizontal estimations of environmental conditions and instability around and over Lake Erie. However, the shallow vertical extent of the MBL resulted in it being poorly represented by the GFS40, with often only one grid point located inside the MBL. This resulted in model-generated MBL wind and temperature profiles that were largely unresolved. Due to the lack of adequate observational data or model output, considerable use of past theoretical and observational studies of similar MBL development and structure were

used to approximate the evolution of the low-level atmospheric vertical profile. This will be described in further detail in Chapter 3.

Chapter 3
Climatology of Storm Interactions with Lake Erie

3.1 Overall Storm Behavior

In order to identify how convective storms are modified as they cross Lake Erie, a climatological analysis of storm/lake interaction over the 2001-2007 period was performed. Since the forcing mechanism for the convection can differ depending on its structure, the study separated convective events into four categories: cluster, isolated, linear, and complex. Each event was classified based on the storm's presentation on radar (refer to Chapter 2). Changes in the intensity of each storm as it moved over the lake were documented using maximum base reflectivity observations at every available radar scan while the storm was over the water surface. This was done to determine patterns of storm strengthening or weakening based on differing convective types and environmental conditions over the lake.

Of the 89 convective events included in the study, 24 were clusters (27%), 20 were isolated (22%), 27 were linear (31%) and 18 were complexes (20%). Figure 7 shows that the overall peak (74%) of convective interaction with Lake Erie occurred in the months of May-August, with the maximum in July. This trend was also seen among the isolated, complex and linear systems; however the maximum occurrence of clusters was in May. Figure 8 shows that in general, convection occurred more frequently in the late afternoon and overnight hours (1400-2200 LST), with a relative minimum in the early morning (0200-0600 LST). Linear systems showed a relative maximum during the late morning and afternoon (1000-1800 LST), while cluster and isolated systems had a relative maximum during the late afternoon and evening (1400-2200 LST). The relative maximum for complexes was observed during the overnight (2200-0200 LST) and morning (0600-1000 LST) hours.

Table 1 shows how convective intensity changed with the amount of time over Lake Erie according to storm type. Overall, less than 10% of storms strengthened over the lake, and no storms exhibited a significant amount of strengthening (>+8 dBZ) at either 30 or 60 minutes (denoted +30 and +60 mins, respectively) over the water. Examination of convective behavior at +30 mins shows that all four convective types behaved similarly. A majority (55%) of all convection experienced no change (-2/+2 dBZ) at +30 mins, with smaller percentages (29% and 8%) of all storms experiencing moderate weakening (-3/-7 dBZ) and significant weakening (>-8 dBZ), respectively.

Noticeable differences in storm behavior are seen at +60 mins. The linear (48%) and complex (50%) systems had a higher percentage of events that experienced no change in maximum reflectivity than cluster (25%) and isolated (25%) events. While the percentages that experienced moderate and significant weakening are similar for all types, a higher percentage of cluster (25%) and isolated (35%) storms died over the lake than linear (7%) and complex (6%) systems.

The same trend of weakening is seen in the average maximum reflectivity change at +30 and +60 mins (Table 2). Average reflectivity change is determined by linearly averaging the reflectivity change value observed at a given time over water (TOW) for all cases of a particular convective type. Cases which have fallen below 45 dBZ or moved over the downwind shore were not included in the average calculations, meaning the average values presented here are likely underestimates. At +30 mins, the average reflectivity change was slightly negative for all four types, and standard deviations of the changes were similar. However, at +60 mins the average reflectivity change was much more pronounced for clusters (-4.33 dBZ) and isolated (-3.73 dBZ) events than linear (-1.57 dBZ) and complex events (-1.69 dBZ).

Taken together, the statistical characteristics of storm evolution over Lake Erie suggest that linear and complex systems react differently when they propagate over the lake for up to 60 minutes than cluster and isolated events. It also appears that convection must be over the lake for at least 30 minutes in order for systematic changes in their intensity to occur, regardless of type.

3.2 Analysis of Environmental Parameters

The effect of Lake Erie's MBL on convection is worthy of further examination. Since near-surface instability is often a factor in controlling convective intensity, lake-induced changes in near-surface instability were examined to identify potential relationships with storm intensity changes. Since near-surface instability observations were available only at KDTX and KBUF every 12 hours, surface temperature data were used to infer changes in instability. Hourly surface temperature observations taken from around and over Lake Erie were used to create several parameters of temperature change associated with the water surface. These parameters were then used to identify statistical relationships to storm intensity changes over the lake.

A parameter measuring the surface temperature difference between the over-lake air temperature and upwind over-land temperature (LAT-UWT) and was used to diagnose changes in near-surface instability. A parameter measuring the difference between the lake water temperature and over-lake air temperature (LT-LAT) was used to diagnose the instability of the MBL (refer to Appendix C for parameter definitions). These parameters were then compared to observed changes in maximum reflectivity at +60 mins, since a large percentage of storms did not reveal any noticeable intensity changes at +30 mins (Table 1).

Figure 9 shows the changes in storm maximum reflectivity (at +60 mins) with respect to the difference between surface air temperature over Lake Erie and the surface air temperature over the upwind land (LAT-UWT) for each of the four convective types. Isolated systems (Figure 9b) showed a trend of increased weakening with increasingly-colder lake air temperatures (LATs) relative to the land (down to 8^{o}C colder). Cluster systems (Figure 9a) appeared to weaken more as the LATs became closer to the over-land air temperature, including when the LAT was warmer. However, there is a high variability in the cluster data, and this trend is dependant on the potential outlier of a -14 dBZ change associated with a +2^{o}C change in surface air temperature over the lake. No definitive relationship between changing surface air temperature and storm behavior is evident for the linear (Figure 9c) and complex (Figure 9d) systems.

Isolated storms appear to have exhibited a slightly negative trend between MBL instability (LT-LAT) and maximum reflectivity (Figure 10b). However, this relationship is dependent on two data points where the MBL is unstable (LT-LAT +) and therefore may not be representative of the actual relationship. A negative relationship is also seen for cluster systems (Figure 10a), although also with a high degree of variability. No relationship is evident between changes in maximum reflectivity (at +60 mins) and MBL instability for linear and complex storms (Figures 10c,d).

To quantify the potential relationships seen in Figures 9 and 10, correlations between maximum reflectivity changes (+60 mins) were determined for a range of measures thought to be related to the surface-based instability over the lake. These include differences in surface-based instability from land-to-lake, and differences between the convective cold pool temperature (CPT) and the over-lake air temperature (CPT-LAT). Lake air temperature (LAT) and

LAT-UWT were the parameters chosen to represent the changes in surface-based instability over the lake, while LT-LAT was chosen characterize MBL instability. The difference in surface air temperature from observation stations located inland upwind and downwind of Lake Erie (UWT-DWT) was also chosen to examine if storms were more correlated to synoptic scale changes in instability compared to land/lake differences.

Resulting correlations between reflectivity trends and the parameters discussed above are shown in Table 3; statistical significance was determined for a value of α=.05. The only statistically-significant relationship is seen between isolated convection and MBL instability (-.65). While this correlation is strongly influenced by two potential outliers in the data set (Figure 10b), it suggests that the more stable the MBL, the less isolated storms decreased in intensity. No other statistically significant correlations are seen, suggesting that a single surface-based variable may not be responsible for storm behavior over Lake Erie.

While no other statistically significant correlations are seen, there are general trends worth noting. The correlation between LT-LAT and maximum reflectivity change was negative for all storm types, further suggesting that a strongly stable MBL contributed to decreased storm weakening. This suggests that in cases in which the MBL is strongly stable (hypothesized as >2.5^{o}C in Graham et al. 2004) storms may have become elevated, did not ingest MBL air, and therefore were not significantly affected by the MBL (Graham et al. 2004). In addition, the correlation value between CPT-LAT and storm intensity change is positive for all storm types, indicating the colder the storm's cold pool was relative to the air over the lake, the more likely a storm's intensity decreased. This suggests that in instances where the cold pool was colder than the MBL, the MBL was lifted by the cold pool and ingested into the convection, leading to storm weakening.

Since storm behavior over Lake Erie does not appear to be controlled by one atmospheric variable, relationships between storm intensity (at +60 mins) and combinations of two stability parameters were investigated. Correlations were calculated between maximum reflectivity changes and the stability parameters after the data had been separated into cases where instability increased/decreased over Lake Erie (LAT-UTW +/-), and whether the MBL was unstable/stable (LT-LAT -/+). These correlations are presented in Table 4.

In cases when there was an increase in surface instability present over Lake Erie (LAT-UWT +, Table 4a), the maximum reflectivity change of complex systems exhibited a statistically significant, negative correlation to the amount of instability (LAT-UWT) over the lake, the instability of the MBL itself (LT-LAT), and synoptic scale instability (DWT-UWT). It should be noted that the small sample size (4) may make the correlations values suspect. These results suggest that complex systems are not very sensitive to any single instability parameter, since their maximum reflectivity change is statistically significant for several combinations of parameters, and is negatively correlated despite an increase in instability over the lake. This hypothesis is strengthened by the fact that complex systems showed a statistically significant negative correlation between maximum reflectivity and when instability decreased over the lake as well (LAT-UWT, Table 4b), suggesting complex intensity reacts similarly regardless of weather the surface air temperature increases or decreases over the lake.

Table 4b also shows a statistically significant positive correlation between isolated storm maximum reflectivity and a surface air temperature decrease when moving from the upwind land to over the lake (LAT-UWT -). This shows that isolated storm intensity increasingly decreased the more the instability was reduced over the water, implying that isolated storms are sensitive to

rapid changes in surface instability and are therefore highly susceptible to interaction with Lake Erie.

Examination of correlations between storm reflectivity and parameters organized by when the MBL was unstable (Table 4c) reveal that statistically significant correlations exist with complex systems for LAT (positive correlation) and UWT-DWT (negative correlation). It should be noted that the sample size associated with these correlations is small, but these contradictory results strengthen the argument that complex systems do not react in a systematic way to changes in near-surface instability.

Correlations from when the MBL was stable (LT-LAT -, Table 4d) suggest that while isolated systems were sensitive to reductions in surface instability, their behavior did not show statistically significant correlations in instances where the MBL was stable. However, a correlation value of .48 between LAT-UWT and maximum reflectivity change in cases where the MBL was stable suggests a relationship of decreasing intensity in regard to decreasing over lake stability for isolated systems. No significant correlations were found for storm intensity changes and any combination of atmospheric parameters that were tested for linear or cluster systems.

Since low-level vertical wind shear is also thought to be important to convective maintenance, vertical wind shear data (sfc-3 km and sfc-6 km) from near Lake Erie were gathered from rawinsonde observations at KDTX for each convective case. Figure 11 shows plots of surface-3 km vertical wind shear and corresponding maximum reflectivity change at +60 mins. While cluster, isolated and complex systems showed no strong relationship between storm intensity changes at +60 mins and surface-3 km vertical wind shear, linear systems show a decrease in maximum reflectivity for wind shear values <15 m s^{-1}. A test of correlation between storm maximum reflectivity decrease at +60 mins and surface-3 km wind shear values <15 m s^{-1}

taken from RAOB data at KDTX revealed that the correlation is statistically significant (.53, parenthesis in Table 3). This indicates that linear storms tend to have weakened as surface-3 km wind shear values decreased. This is in agreement with 'RKW Theory' that squall lines should weaken faster in low shear environments, and suggests that changes in intensity for linear systems were related more closely to synoptic conditions than interaction with the MBL. No discernable trend or correlation was evident for any of the four convective types when considering surface-6 km shear (not shown).

The values seen in Tables 3 and 4 suggest storm behavior when interacting with Lake Erie's MBL is not well correlated to one, or even a combination of two, of the parameters chosen for this study. To further examine how multiple factors may influence storm behavior over the lake, 'flowcharts' were created to illustrate how maximum reflectivity changed under several combinations of environmental and MBL conditions. These charts separated convective events by three atmospheric variables, representing changes in surface instability and low-level vertical wind shear. Storms were classified as the fraction of events that died/significantly weakened, moderately weakened, or experienced no change/moderately strengthed (refer to Chapter 2 for behavior definitions). The category of significant strengthening was not included since no storms were observed to strengthen by >7 dBZ over Lake Erie. Since cluster/isolated systems exhibited similar behavior over the lake, as did linear/complex systems (refer to Chapter 3.1), these systems were grouped together in the flowcharts. Flowcharts using maximum reflectivity change at +60 mins are shown because no noteworth intensity change is observed for any of the convective types at +30 mins (Table 1).

Figure 12 shows three flowcharts constructed for all cluster and isolated systems combined. These charts organized all the cluster/isolated cases by noting the number of events

which occurred under a certain set of atmospheric variables. For example, the left side (denoted in red) of Figure 12a shows that 10 cluster/isolated events occurred in instances where the lake air temperature was warmer than the upwind over-land temperature (LAT-UTW +). Of these 10 cases, 2 cases had a MBL that was considered unstable (LT-LAT +) and 8 cases had a MBL that was considered stable (LT-LAT -). Examination of the cases where the LAT-UWT + and LT-LAT - shows there were two events where the lake air temperature (LAT) was warmer than 20^{o}C, and no cases where the LAT was less than 20^{o}C. The flowcharts were organized with what were considered the most favorable convective environments (red) on the far left (i.e. increase in air temperature over lake, unstable MBL, etc.) and the least favorable convective environments (blue) on the far right.

Once convective events were separated by their atmospheric parameters, the corresponding changes in maximum reflectivity (+60 mins) were examined. The fraction of storms which were observed to experience the corresponding changes in maximum reflectivity at +60 mins were displayed in 3 quantities (moderate strengthening or no change / moderate weakening / strong weakening or died) for each combination of variables. These are denoted in black on Figures 12 and 13. It should be noted that the fractions of storm behavior for each parameter combination do not always add to one; this is due to storms moving over the downwind coast before +60 mins. These storms were not included in the analyses.

Figure 12 shows that cluster and isolated storms tended to weaken or die when instability was reduced over Lake Erie. This is evidenced by the high fraction of storms which died or significantly weakened in cases where the lake air temperature was less than the over land temperature (LAT-UWT -), denoted on the right side in Figure 12. Of the twelve combinations of atmospheric parameters associated with decreasing surface air temperature over the lake (blue

section of Figure 12), ten of them show a majority (>.50) of storms died or significantly weakened. This suggests that decreasing instability is the main cause of cluster/isolated storms dying or significantly weakening when LAT >UWT since it was the common parameter in those cases.

The behavior of cluster/isolated storms is less consistent in cases where the environment is convectively favorable (in red, Figure 12). For example, the far left side of Figure 12a shows that half of cluster and isolated events die/significantly weaken despite increasing instability over the lake, the MBL being unstable and the lake air temperature being >20^{o}C. However, half of the storms also experienced no change/moderately strengthened under the same conditions. It should be noted that the sample size regarding convectively favorable conditions is small for most combinations on the left side of Figure 12, so the results may be unrepresentative.

In contrast, Figure 13 shows that linear and complex systems tend to experience no change/moderately strengthen even when conditions over Lake Erie were convectively unfavorable. This is seen as by the high fraction of storms which were observed to have no change/moderately strengthened despite over-lake conditions that were not conducive to convection. In 10 of the 12 parameter combinations featuring reduced over-lake instability (right side, in blue, in Figure 13), a majority of complex/linear systems maintained strength or moderately strengthened. When considering the storm's cold pool interacting with the MBL (Figure 13b), a high percentage of linear/complexes were observed to maintain strength or strengthen despite the over-lake environment being increasingly convectively unfavorable, even when the MBL was expected be lifted by the cold pool and ingested by the convection (CPT-LAT -).

In cases where conditions over Lake Erie were convectively favorable (left of Figure 13), there is no discernable trend that linear and complex storms consistently strengthened or weakened. This strengthens the argument that linear and complex systems were not greatly affected by interaction with the MBL when LAT >UWT, as was suggested by the correlation values for complexes seen in Tables 3 and 4. Isolated and cluster systems, however, appeared to consistently weaken when interacting with a MBL that was increasing convectively unfavorable, particularly when considering surface instability (temperature) decreases from the upwind land to over Lake Erie.

The conclusions drawn from the average maximum reflectivity change suggests that storms, regardless of type, were not strongly affected by interaction with Lake Erie in their first 30 minutes over the water. However, cluster and isolated systems showed a noticeable average decrease in intensity at 60 minutes over the water, a trend that was not seen for linear and complex systems. These conclusions were strengthened by the flowchart analyses, which showed that linear/complex systems did not behave differently regardless of the environmental conditions of Lake Erie's MBL. Conversely, flowcharts of isolated and cluster systems showed that these types experienced a decrease in maximum reflectivity the more convectively unfavorable the environment over the lake was (i.e. combinations of decreased surface air temperature, a stable MBL, etc).

While it appears that there is a clear trend of cluster and isolated storms weakening over the lake, the magnitude of their observed maximum intensity decrease does not appear well correlated to any given parameter, or combination of two parameters, that were chosen for this study. While the results tend to show that cluster/isolated systems will weaken when the over-lake environment is convectively unfavorable compared to the upwind over-land environment,

the correlation results in this study show there is no clear linear relationship between the dBZ decrease (at +60 mins) and the observed LAT, LT-LAT, LAT-UWT or DWT-UWT. However, the correlation analyses do suggest notable trends, including the MBL being ingested and weakening convection when the cold pool was cooler than the LAT, as well as storms possibly becoming elevated in cases of strong MBL stability.

Chapter 4
26 July 2005 Squall Line Case

To better understand processes by which interacting with cooler lakes can modify convection, the case of 26 July 2005 was investigated. On this date, a severe squall line developed in Lower Michigan and propagated eastward, eventually moving over the cooler surface of Lake Erie. While over the lake, the squall line experienced changes in its kinematics and structure, forming two small-scale bow echoes over the lake, and producing severe surface winds.

4.1) Environmental Conditions

At 1500 UTC, a low pressure center was located over the northern lower peninsula of Michigan, with a cold front stretching southwest through Michigan and a warm front extending eastward into Ontario, Canada (Figure 14). The convection developed in the warm sector in an area of strong warm air advection (surface wind ~210^{o} at 7-10 m s^{-1}) and high surface-based instability (~2500-3000 J kg^{-1}, as determined from the 1800 UTC GFS40 model initialization). 1200 UTC RAOB observations from Wilmington, OH (KILN) (Figure 15a**),** located upwind from Lake Erie relative to the 0-3 km mean synoptic wind (248^{o} @ 16 m s^{-1}), show a most unstable CAPE (MUCAPE, defined as the most unstable parcel in the lowest 300 mb) value of 1398 J kg^{-1}. This was significantly higher than the instability present at KDTX (625 J kg^{-1}) and KBUF (0 J kg^{-1}). Also worth noting from Figure 15a is the significant amount of dry mid-level air seen in the KILN sounding (around 600 mb), which was not present at KBUF at 1200 UTC (Figure 15b). This suggests that the air being advected into the Lake Erie region during the afternoon was drier at the mid-levels and contained increased instability above

the surface. The numerical modeling results from Parker (2008) suggest that dry mid-level air can negatively effect squall line intensity when interacting with surface cool layers.

Rawinsonde soundings (Figure 15b,c) from KBUF and KDTX at 1200 UTC (closest to the time of convective initiation) indicated approximately 15 and 20 m s^{-1} of surface-2.5 km U-wind shear, respectively. VAD shear profiles determined from WSR-88D Level III data, accurate to approximately 2 m s^{-1} (Collins 2001), show ~21 m s^{-1} of surface-2.5 km U-wind shear at KDTX at 1700 UTC (time of convective initiation near Detroit) and ~19 m s^{-1} at KCLE at 1900 UTC (ahead of the convective precipitation at Cleveland). These shear values are comparable to those found in previous observational (Coniglio et al. 2004, their Figure 18) and numerical modeling (Weisman and Rotunno 2004, their Table 1a) studies of squall lines that formed bow echoes. These studies also showed that bow echoes are likely with instability (>2500 J kg^{-1}) and surface-2.5 km shear values (~20 m s^{-1}) observed on this date.

4.2) Lake Modification of the Atmosphere

Surface air temperatures in northern Ohio and western Michigan were ~31-32^{o}C at 1700 UTC; data from buoys 45005 and 45132 in Lake Erie (Figure 6) show the water temperature was ~ 26^{o}C. As a result, a cool mesoscale airmass formed over Lake Erie in response to the cooler water surface. This airmass can be clearly identified by the trough in the surface temperature field over and downwind (north/northeast) of Lake Erie in Figure 16. The lake-modified air is considered the marine boundary layer (MBL) in this study.

Since lake breeze circulations (LBC) are often observed in the Great Lakes region during the warm season (i.e. Lyons 1972, Laird et al. 2001), and these may influence convective evolution, the presence of a LBC was investigated. Examination of surface wind and

temperature data along the coastline of Lake Erie as well as radar data from KCLE and KDTX from the afternoon of 26 July 2005 revealed no evidence of a LBC. Calculation of the lake breeze index, ε, (equation 1) using surface observations taken from Mansfield, OH (KMFD) at 1800 UTC as the inland station revealed $\varepsilon \approx 17$, well above the usual criterion for sea-/lake-breeze formation of ≤3.0 (Laird et al. 2001). KMFD was chosen as the reference inland surface air temperature due to its location upwind of Lake Erie based on the synoptic wind, as well as its agreement with the regional temperatures throughout inland Ohio (Figure 16). The value $\varepsilon \approx 17$ is in agreement with the lack of evidence of a LBC on this date, primarily due to strong surface winds (~7-9 m s^{-1}). With the absence of a LBC, the cooler airmass over and north of Lake Erie suggests that the MBL in this case could be considered an internal boundary layer (IBL) which formed as the convective boundary layer (CBL) over land was advected over the cooler water by the synoptic wind (refer to Garratt 1990 for IBL review). This classification allows us to use previous IBL theory and observations in developing an understanding of how the MBL interacted with the convection.

4.2.1) Characterization of the Marine Boundary Layer

In order to estimate the temperature profile of the MBL and further understand how it altered the atmosphere encountered by the squall line, the IBL stability parameter **S** (equation 2) derived by Smedman et al. (1997a) was employed. Surface observations from 1800 UTC were used to approximate environmental conditions over all of Lake Erie closest to when the squall line approached the lake. Fetch of each location over Lake Erie was determined as the along-

wind distance to the southern shoreline using an average surface wind[2] direction of 210°. Calculations show ***S*** ranged from ~40 over southern Lake Erie to ~55 over northern Lake Erie. Therefore, the MBL was characterized as a *statically stable* IBL (Smedman et al. 1997a) for this study.

Previous dimensional analysis (Mulhearn 1981) and numerical modeling studies (Garratt 1987) assert that IBL depth can be approximated by equation (3). This relationship was used to estimate MBL depth at a series of grid points constructed over Lake Erie for 26 July 2005, shown in Figure 17.

Figure 17 shows that the MBL was estimated to reach a maximum depth along Lake Erie's northwest coastline. Relative to the squall line motion (white dotted line in Figure 17), the MBL was estimated to be at its maximum depth of ~125 m near Erieau, Ontario (CWAJ, Figure 6) decreasing steadily toward the east. This analysis suggests the squall line would encounter a statically stable MBL of continually lower depth as it moved eastward across the lake.

The presence of the MBL affected the amount of surface-based potential instability. GFS40 1200 UTC initialization model forecasts of surface-based CAPE and most unstable CAPE (MUCAPE) at 1800 UTC were both 2847 J kg^{-1} for KDTX and 2600 J kg^{-1} for KCLE. This suggests significant instability was present west and east of the lake. Model soundings over Lake Erie (Point A in Figure 6) indicated 824 J kg^{-1} of CAPE, meaning surface-based instability was still present but reduced by ~2000 J kg^{-1}.

The MBL potentially altered the near-surface environment encountered by the squall line in other ways. The presence of the cooler airmass would be expected to alter the vorticity

[2] Observed surface wind speed (Vs) is used instead of the geostrophic wind (Vg) in order to better capture the actual conditions of IBL formation. Since Vs<Vg, this increases S values calculated in this study; since S<75 in this case, this further strengthens the argument that the IBL is statically stable.

generated by the squall line's cold pool by altering the buoyancy gradient between the cold pool and the ambient environment near the surface. Due to the changing depth of the MBL encountered by the squall line as it moved eastward (Figure 17), as well as changing surface air temperatures inside the MBL (Figure 16), the buoyancy gradient was expected to be constantly changing as the convection moved through Ontario (decreasing) and over Lake Erie (increasing). This potentially induced changes in the squall line per RKW Theory. Additionally, the changes in surface friction from the land to water were also expected to affect the squall line by reducing the amount of cold pool vorticity generation lost to frictional mixing (Fankhouser et al. 1992)

4.2.2) Alteration of Vorticity Generation by the MBL

Since the role of ambient vorticity generation has been shown in numerical modeling studies (i.e. RKW, Bryan et al. 2006) to impact squall line intensity, it is important to understand how the presence of the MBL potentially alters the horizontal vorticity generation of the system. The 2D Boussinesq, inviscid vorticity (η) equation is defined as:

$$\rho_o \frac{d}{dt}\frac{\eta}{\rho_o} = -\frac{\partial B}{\partial x} \qquad (4) \qquad \text{where} \qquad \eta \equiv \frac{\partial u}{\partial z} - \frac{\partial w}{\partial x} \qquad (5)$$

and B is the total buoyancy. To examine the potential vorticity generation of buoyancy gradients introduced by the presence of the MBL relative to the west-to-east squall line motion, we integrate equation (4) from a point on the west (left along the white dashed line in Figure 17, L) to a point on the east (right, R), and from the ground to the MBL top (T_M). Previous observational (i.e. Doran and Gryning 1987, Angevine et al. 2006), and numerical modeling (i.e. Smedman et al. 1997a) studies of stable IBLs have found they often exhibit a linear potential temperature profile with height. Therefore, we use a linear buoyancy profile $B_{min}(1\text{-}h/T_M)$,

where B_{min} is the minimum buoyancy acceleration in the MBL and *h* is a height inside the MBL. Equation (4) then becomes:

$$\frac{\partial}{\partial t}\int_{L}^{R}\int_{0}^{T_M}\eta dx dz = \int_{0}^{T_M}\left[B_{\min}\left(1-h/T_M\right)\right]dz_L - \int_{0}^{T_M}\left[B_{\min}\left(1-h/T_M\right)\right]dz_R. \qquad (6)$$

Since the MBL formed in response to forcing by the cooler lake surface, we assume that B_{min} is at the surface. Average surface buoyancy can be approximated as:

$$B_{\min} \equiv g\left[\frac{\Delta\theta}{\bar{\theta}} + .61(q_v - \bar{q}_v) - q_c - q_r\right] \qquad (7)$$

where $\boldsymbol{g}$ is acceleration due to gravity, $\bar{\theta}$ is the potential temperature of the ambient environment, $\Delta\theta$ is the temperature difference between the ambient environment and the lake surface, and $\boldsymbol{q_v}$, $\boldsymbol{q_c}$, and $\boldsymbol{q_r}$ are water vapor, cloud water and rainwater mixing ratios, respectfully. The ambient environmental potential temperature (~305 K) was estimated by averaging surface observations taken at four locations (KTOL, KCLE, KERI, KDKK) located on the southern and eastern shore of Lake Erie (Figure 6). This represents the surface air temperature over land that was being advected over the water surface. Surface water temperature is taken as the average water temperature recorded at buoys 45005 and 45132. Water vapor mixing ratios are approximated from surface dew points, and the mixing ratio in the MBL is assumed to be equal to the air over the land (~18 g kg^{-1}). No clouds were observed over the lake prior to convective interactions, so we set cloud water and rainwater mixing ratios to zero. Based on these approximations, the average surface buoyancy over Lake Erie at 1800 UTC was ≈ -.143 m s^{-2}. Using this value for B_{min} in equation (6) gives us:

$$\frac{\partial}{\partial t}\int_{L}^{R}\int_{0}^{T_M}\eta dx dz = \int_{0}^{T_M}\left[-.143\left(1-h/T_M\right)\right]dz_L - \int_{0}^{T_M}\left[-.143\left(1-h/T_M\right)\right]dz_R. \qquad (8)$$

The estimated depth of the MBL (equation 3) at two successive east-west grid points (Figure 17) was used to determine the horizontal vorticity tendency. The results (Figure 18)

indicate that on this date there would have been positive vorticity tendency over portions of western Lake Erie and shoreline areas to the north of the lake, while much of the eastern portion of the lake would have exhibited negative vorticity tendency.

The vorticity tendency field (relative to squall line motion) in Figure 18 can be attributed to the changes in the MBL height from west-to-east over the lake. As can be seen in equation (3) and Figure 17, the MBL is expected to achieve its maximum depth at the point where the overwater fetch is greatest. This results in maximum MBL depth, and therefore maximum negative integrated total buoyancy, occurring near Lake Erie's northern shoreline. The negative integrated total buoyancy then decreases toward the east as the depth of the MBL decreases.

The along-line vorticity field of the MBL over Lake Erie depends critically on the ambient wind and storm motion direction; each wind/storm motion pairing will create a different along-line vorticity profile of the MBL.

4.3) Squall Line Evolution

Convection developed along pre-existing outflow boundaries in southern Michigan ~1700 UTC (Figure 14). It initially developed as scattered individual cells (Figure 19a) which moved toward the north-northeast (215^{o}) in accordance with the surface-500 hPa mean wind (not shown). Convective cells continued to develop, eventually combining to form the squall line, consistent with a 'broken areal' formation as designated by Bluestein and Jain (1985). Figure 19b shows the early stages of the squall line, which contained a continuous line of >50 dBZ reflectivity, had a southwest-to-northeast orientation, and moved due east (90^{o}). It is important to note that convection continued to develop to the south and west of the original squall line

(Figure 19b); only convection associated with the original squall line was considered for the current investigation.

Figure 20a shows a storm relative velocity (SRV) cross-section through the squall line at 1822 UTC, shortly after a continuous line of convection emerged (Figure 19b). The SRV field shows a fairly erect front-to-rear (red) flow at the leading edge of the storm; nearly horizontal front-to-rear flow (>13 m s^{-1}) is observed above ~7600 m behind the leading edge. Rear-inflow is evident, denoted in green, which increases from ~3 m s^{-1} near the back of the system (left side) to ~15 m s^{-1} near the leading edge. As the storm was approximately 85-100 km away from the KCLE radar, there were no observations below approximately ~1000 m, preventing observational analysis of the flow near the surface.

The southern end of the squall line was the first to reach Lake Erie at approximately 1830-1835 UTC. Figure 19c shows that at 1853 UTC, shortly after moving over the water, a small-scale bow echo developed on the southern end of the squall line. Examination of the SRV field (Figure 20b) shows that the erect front-to-rear flow at the leading edge of the storm was no longer evident, suggesting that the updraft of the squall line had become tilted. The rear-inflow also strengthened to a maximum of >20 m s^{-1} and became shallower within the squall line. As would be expected with the rearward-tilting of the updraft, there is an observed weakening of the convection on the southern end which can be seen by a decrease in base reflectivity values (Figure 19c) as well as a rearward expansion of >45 dBZ reflectivities.

The northern section of the squall line reached the lakeshore ~1850 UTC. Figure 19d shows another small-scale bow echo developed in the northern portion of the line by 1913 UTC, almost immediately after that section of the squall line moved over the lake. At the same time, the southern bow echo continued to expand, and a well-defined outflow boundary was observed

in the base reflectivity (Figure 19d). A SRV cross-section through the southern bow by 1913 UTC (Figure 20c) suggests that the updraft remained tilted and the rear-inflow appeared to sink toward the surface behind the leading edge of the convection. The tilting of the updraft rearward, convective weakening and possible descent of the RIJ have been shown in numerical modeling studies (RKW, Weisman and Rotunno 2004) to be products of the cold pool's vorticity overwhelming the environmental vorticity, resulting in the cold pool pushing forward at the surface.

Figure 21 shows the height of the top of the rear-inflow, defined for this purpose as the top of the <-3 m s^{-1} SRV layer, at three distances (15 km, 45 km, and 75 km) behind the leading edge of the squall line spanning the timeframe of the storm's movement from land to water. After crossing the shoreline, the rear-inflow appeared to steadily decrease in height. Note that several velocity criteria were examined and all showed a similar pattern of decrease in height. This descent is consistent with the numerical modeling results of RKW, Weisman (1993) and Weisman and Rotunno (2004), which showed RIJ descent when the vorticity of the cold pool overwhelms that of the ambient environment and accelerates.

In addition to the observed changes in several areas along the squall line, mean characteristics of the system also changed. Mean squall line motion increased by ~7 m s^{-1} as the convection moved from land to water **(**Figure 22). This suggests the reduction of frictional mixing is another potential cause of the cold pool acceleration (and updraft tilting) over the lake, in addition to the hypothetical increase in cold pool strength caused by a reduced buoyancy gradient. As a result of the tilting, the intensity of the convection decreased over Lake Erie. Figure 22 shows a time series of average maximum base reflectivity for the squall line as it

moved through southern Ontario and over Lake Erie. A decrease in the maximum reflectivity is observed as the storm moved from land to water.

4.4) Potential Effect of Lake Erie and the MBL on the Squall Line

RKW used equations (4) and (5) to derive an ideal relationship between environmental and cold pool horizontal vorticity generation which leads to maximum squall line intensity. They integrate equation (4) from a point inside the cold pool (P) to a point in the ambient environment (E), from the ground to the top of the cold pool (T_P), and solve the equation where the system is in balance$\left(\frac{d\eta}{dt}=0\right)$. They then assume 1) there are no horizontal changes in vertical motion away from the immediate cold pool edge: $\frac{\partial w}{\partial x}\approx 0$, and 2) negligible ambient buoyancy: $B_E \approx 0$. Weisman (1992) added a term to account for vertical wind shear in the cold pool, leading to:

$$\Delta u_E^2 = c^2 - \Delta u_P^2 \qquad (9) \qquad \text{where} \qquad c^2 \equiv 2\int_0^{T_P}(-B_P)dz\,, \qquad (10)$$

And Δu_E is storm-relative ambient vertical wind shear over the height of the cold pool, Δu_P^2 is vertical wind shear inside the cold pool ($u^2{}_{P,Tp} - u^2{}_{P,0}$) and B_P represents the buoyancy of the cold pool (c) (RKW, section 4). Equation (9) is what RKW refers to as the 'optimal state,' where the generation of negative vorticity by the cold pool (right side of equation 9) is balanced by the import of positive vorticity by the ambient environment (generated by storm-relative vertical wind shear, Δu_E). In addition, Fankhouser et al. (1992) concluded that frictional mixing at the surface reduces the negative vorticity produced at the leading edge of the cold pool, and

should be included in the system's vorticity balance relationship. Adding the friction mixing term $\frac{\partial^2 \overline{u'w'}}{\partial z^2}$ to the 'optimal state' renders (Fankhouser et al. 1992):

$$\Delta u_E^2 = c^2 - \Delta u_P^2 + 2\int_L^R \left(\left. \frac{\partial \overline{u'w'}}{\partial z} \right|_{Tp} - \left. \frac{\partial u'w'}{\partial z} \right|_0 \right) dx. \qquad (11)$$

$$\underbrace{}_{1} \quad \underbrace{}_{2} \quad \underbrace{\phantom{+ 2\int_L^R \left(\left. \frac{\partial \overline{u'w'}}{\partial z} \right|_{Tp} - \left. \frac{\partial u'w'}{\partial z} \right|_0 \right) dx.}}_{3}$$

The right side of equation (11) describes the vorticity production of the cold pool: term 1 represents production due to the buoyancy gradient between the cold pool's leading edge and the ambient environment; term 2 represents production from vertical shear inside the cold pool, and term 3 represents frictional mixing caused by the cold pool's interaction with the surface (reduces vorticity production).

The presence of Lake Erie and its associated MBL on 26 July 2005 is expected to have altered the circulation balance between the cold pool and ambient environment. By changing the buoyancy of the ambient environment, as well as introducing changes in surface friction, the vorticity produced at the leading edge of the cold pool is expected to change, potentially inducing changes in the convective kinematics and structure.

4.4.1) Squall Line Evolution

Figure 23 shows a conceptual diagram of the squall line as it moved eastward. At 1800 UTC the squall line was over land in southern Ontario (point A in Figure 23a); it had not yet encountered the cooler air associated with the MBL. At this stage term 1 in equation (11) is determined by the buoyancy gradient at the leading edge of the cold pool relative to the ambient environment (~ -.34 m s^{-2}), and terms 2 and 3 are the vertical shear inside the cold pool and

frictional mixing over the land, which could not be measured by the available operational observation platforms used for this study.

As the storm moved closer to Lake Erie at 1830 UTC (point A to B in Figure 23b), it encountered the MBL airmass which became increasingly cooler near the surface as the storm moved east toward the lakeshore (Figure 16). Figure 23b shows that relative to the storm path (dotted line in Figure 17) the surface air temperature decreased to 299 K at CWAJ, which is also where the MBL is estimated to have reached its maximum depth of ~125 m (Figure 17). This suggests that the cold pool was interacting with a MBL of increasing negative vertically-integrated buoyancy as it moved across southeastern Ontario and reached the lakeshore at CWAJ. As a result, term 1 in equation (11) was expected to continually decrease as the buoyancy gradient at the leading of the cold pool steadily decreased, reducing cold pool vorticity generation.

In association with the move into progressively cooler MBL air (Figure 23b), the squall line was observed to undergo a 3 dBZ (Figure 22) increase in average maximum base reflectivity in ~15 minutes (1812-1827 UTC), despite a perceived decrease in surface CAPE associated with the cooler MBL air. The convection also was observed to undergo a decrease in forward speed of approximately 5 m s^{-1}. These observations are in agreement with the numerical modeling results from Parker (2008) for simulated squall lines interacting with a surface cool layer. In his study, simulated squall lines reached a second maximum in updraft intensity, despite the decrease in surface CAPE, and underwent a reduction in forward speed as the cold pool moved into an increasingly cooler surface layer. Parker (2008) referred to this as the "stalling" stage, and hypothesized it was in response to the cold pool strength decreasing toward the optimal ratio with the ambient shear, in agreement with RKW principles.

As the squall line moved from land eastward over Lake Erie (point B to C in Figure 23c), the surface air temperature of the MBL was observed to increase to ~301 K over the center of Lake Erie (along the storm path, Point A in Figure 6), increasing the temperature difference at the leading edge of the cold pool. This, combined with the decreasing depth of the MBL as the convection crossed the lake (Figure 17), would be expected to increase the circulation generated at the leading edge of the cold pool (term 1 in equation 11). Additionally, the decrease in surface friction associated with the cold pool moving from land to water would be expected to decrease term 3 in equation (11), hypothetically also leading to an increase in cold pool vorticity generation.

Evidence of the cold pool circulation overwhelming the shear is observed. Figures 19c,d show small-scale bow echoes formed in correlation with the convection reaching the water surface, as well as a noticeable outflow boundary accelerating southward from the convection. In accordance, SRV cross-sections in Figures 20b,c show the squall line's updraft became increasing tilted (front-to-rear flow) as the storm moved over the water. Additionally, Figure 22 shows that the convection was observed to undergo a rapid increase in forward speed (~ 7 m s^{-1}) during the time period where the storm moved from land to water.

The squall line was also observed to undergo a steady decrease in maximum average reflectivity in the first ~60 minutes over the water (Figure 22). However, the reason for this decrease in intensity cannot be confirmed from the observations in this study. While the decrease in average maximum reflectivity appears significant compared to when the storm was at its maximum intensity shortly before moving over the water (~ 6 dBZ), it should be noted that this average maximum intensity occurred during what is believed to be the squall line's 'stalling'

stage (Parker 2008). In relation to the intensity of the convection before interacting with the lake-cooled air (50 dBZ at 1807 UTC), the decrease in intensity is approximately 3 dBZ.

Parker (2008) showed that simulated squall lines can maintain their intensity and remain surface-based when encountering surface cool layer (despite increases in CIN) as long as the temperature gradient at the leading edge of the cold pool is strong enough to promote sufficient lifting. The observations in this case suggest that the temperature gradient was 4 K when the cold pool reached the lake shore, and increased to 6 K when the squall line was over the middle of Lake Erie. These gradient values fall within the values which provide sufficient lifting in Parker (2008), suggesting that the increased CIN over the lake may not be responsible for the observed intensity decrease. Given the strong negative correlation between the average maximum intensity decrease (Figure 22) and observed increase in storm motion, as well as evidence of the updraft becoming tilted, it is possible that the decrease in intensity is due to the cold pool circulation becoming stronger than that generated by the ambient shear. This would work to pull the updraft rearward (relative to the squall line) and therefore reduce the vertical intensity of the updraft.

As viewed in Table 5 (in correlation with Figure 23), the observed changes in the squall line while approaching and over Lake Erie are hypothetically caused by changes in friction, as well as changes in the cold pool's buoyancy gradient (and therefore cold pool strength) approaching/over the water. However, solid conclusions as to the relative importance of each mechanism of the decrease in intensity while over the lake are not obtainable from the limited data available for this study.

Chapter 5
Conclusions and Discussion

5.1 Climatological Storm-Lake Interactions

In order to identify how convective storms are modified as they cross Lake Erie, an analysis of pre-existing convection crossing the lake for the 2001-2007 time period was conducted. Convective events where identified using radar data as having a maximum reflectivity of >45 dBZ prior to moving over the water, and were tracked until either their maximum reflectivity fell below 45 dBZ or the convection crossed the downwind shore. Events were then separated into one of four categories based on horizontal convective structure: cluster, isolated, linear or complex. Their maximum reflectivity changes were separated into the following categories based on the magnitude of dBZ change: significant strengthening (≥ +8 dBZ), moderate strengthening (+3 to +7 dBZ), no change (+2 to -2 dBZ), moderate weakening (-3 to -7 dBZ), significant weakening (≥ -8 dBZ) and died (max reflectivity <45 dBZ). Changes in maximum dBZ were recorded at 30 (+30 mins) and 60 minutes (+60 mins) after moving over the water.

In total, 89 convective cases were identified: 24 clusters, 20 isolated, 27 linear and 18 complexes (Figure 7). The maximum number of convective systems occurred in the late spring/summer months, with a maximum in July. Linear and complex systems showed a relative maximum in July, while cluster occurrence peaked in May and isolated storms peaked in July and September. Regarding the time of day at which the convection reached the lake (Figure 8), the maximum was during the late afternoon (1400-1800 LST); this time-of-day maximum was also observed for isolated systems. Linear systems showed a relative maximum during the late morning/afternoon (1000-1800 LST), clusters during the evening (1400-2200 LST) and complex systems during the overnight and early morning hours (2200-0200, 0600-1000 LST).

Analyses of how convective intensity changed with time (Table 1) revealed that at +30 mins changes were generally minimal. Less than 10% of the storm systems showed some strengthening over the lake, and no storms exhibited a large amount (maximum reflectivity change of at least +8 dBZ) of strengthening. A majority of storms (ranging from 45% for isolated to 63% for clusters) had no change, with a smaller percentage (≥40%) of all types had moderate weakening. The percentage of storms that experienced significant weakening or died at +30 mins was less than 10% for all types.

Noticeable differences in storm behavior were observed at 60 minutes over the water. No storms experienced strengthening. Nearly half of the linear and complex systems showed no intensity change, while only 25% of isolated and cluster systems showed no change. Conversely, a larger percentage of cluster (25%) and isolated (35%) systems died at +60 mins, while <10% of linear and complex systems died. This trend is also seen in the average maximum reflectivity changes at +60 mins, as the average reflectivity change for cluster (-4.33 dBZ) and isolated (-3.73 dBZ) systems is approximately double the change observed for linear (-1.57 dBZ) and complex (-1.69 dBZ) systems (Table 2).

These results indicate that convection did not significantly strengthen while over the lake, and a large majority, regardless of type, experienced either no change or moderate weakening at 30 minutes over the water. However, at 60 minutes over the water, a large majority of cluster and isolated systems either weakened or died, while a majority of linear and complex systems experienced no change. This suggests that cluster and isolated systems are sensitive to interaction with Lake Erie's MBL and tend to weaken, while linear and complex systems are not as sensitive to moving over the water.

Flowchart analyses (Figures 12 and 13) were created to illustrate how cluster/isolated and linear/complex storms behaved under varying combinations of three study parameters. The results showed that isolated/cluster storms tended to weaken more in combination with a convectively unfavorable environment (i.e. stable MBL, cooler over-lake surface air temperature, and decreased surface air temperature over the lake relative to the upwind land). Linear/complex systems did not show a preference for weakening regardless of the over-lake surface conditions.

The general trend appears to be that cluster/isolated systems weaken when encountering a convectively unfavorable environment over the lake. However, correlations between maximum reflectivity decrease and specific over-lake instability parameters were not significant, suggesting that the decrease in storm intensity does not exhibit a linear correlation to any one (Table 3), or combination of two (Table 4), over-lake parameter(s) tested in this study. Conversely however, the negative correlations between maximum reflectivity change and MBL stability for all systems suggests that strongly stable MBLs contributed to a decrease in the amount of storm weakening. This relationship supports the previous hypothesis of Graham et al. (2004) that in cases of strong MBL stability (LT-LAT -2.5^{o}C in Graham et al. 2004) convection becomes elevated (not ingesting near-surface air), and is not affected by the MBL.

An observed statistically-significant positive correlation between maximum reflectivity change and 3 km wind shear >15 m s^{-1} for linear systems is in agreement with RKW theory and suggests that linear system intensity may be more sensitive to synoptic conditions than lake-induced changes. However, the MBL and water surface may affect linear systems in other ways, such as causing changes in their convective structure and air flow within the system. These alterations can have important effects, such as severe surface winds developing as a result of

higher momentum air within the system being pulled downward (i.e. Weisman 1992). These potential changes to the squall line are likely related to factors (decreased surface friction over water surface, reduction of cold pool strength due to a cooler ambient environment) other than the decrease of surface-based instability examined in this climatology, as discussed in the case study of 26 July 2005 (Chapter 4).

It should be noted that while the low correlation values in this study suggest that storm intensity changes are not well linearly correlated with the over-lake parameters used in this study, it does not mean that they are not related. Future work should use non-linear statistical methods, or analysis which group several parameters together, to attempt to identify relationships between over-lake conditions and storm behavior. Also, the climatological data base should be expanded to include more years as data becomes available, as several parameter/intensity change relationships had small sample sizes, likely obscuring any potential relationship that exists. Additionally, higher resolution observations (both spatial and temporal) are needed of the low-level environment over Lake Erie. RAOB data would be particularly useful to help gain additional insight into the stability profiles inside the MBL, as well as how the MBL alters low-level wind shear and surface-based instability.

5.2 The 26 July 2005 Squall Line Case

Investigation of the squall line case which occurred on 26 July 2005 revealed that the convection encountered changes in both ambient buoyancy (interaction with the MBL) and surface friction (movement from land to water surface) as it progressed from southern Ontario to over Lake Erie. The squall line was observed to undergo strengthening and a slowing in forward motion as it approached the lake, followed by a consistent decrease in maximum reflectivity and

increase in forward speed once it moved over the water. Furthermore, radar analysis of the storm revealed that two small scale bow echoes developed and the convective updraft became noticeably tilted (front-to-rear flow) in correlation with the movement from land to water. The observational results of this study appear to be in agreement with the proposed effect of frictional mixing on the squall line (Fankhouser et al. 1992), as well as previous numerical modeling studies of squall lines moving over a cooler surface (L07) and interacting with a surface cool layer (Parker 2008). Additionally, the changes in squall line intensity and structure appear to follow the basic principles of cold pool/ambient vertical wind shear circulation (im)balance of RKW Theory.

Analyses of the cold pool/ambient shear ratio suggested by RKW for conditions the storm encountered as it crossed southern Ontario indicated that a period of brief strengthening would be anticipated. As the squall line moved toward the lake, it encountered an MBL that became both cooler at the surface (Figure 16) and deeper (Figure 17). This is hypothesized to have steadily decreased the temperature gradient at the leading edge of the cold pool, reducing the cold pool strength (Figure 23b). According to RKW principles, this would tend to cause the system to become closer to circulation balance, providing a more vertical updraft and leading to an intensification of the convection.

Parker (2008) observed this behavior in numerical simulations of squall line interaction with cool surface layers. He deemed the 'stalling stage' as the period where the convection briefly intensified and slowed in association with the reduction of the cold pool temperature gradient, in agreement with basic RKW principles. Observations of the 26 July 2005 case show the convection underwent a 'stalling' period as it approached Lake Erie's northern shoreline.

The convection also exhibited a ~3 dBZ increase in average maximum reflectivity and a ~5 m s^{-1} slowing was observed (Figure 22).

When the squall line moved from land to over water, several key changes in its structure and intensity were observed. Observations of base reflectivity showed that two small-scale bow echoes developed on the northern and southern ends of the line almost immediately after the convection moved over water (Figure 19c,d). In correlation with bow echo formation, cross-sections of radar-derived storm relative velocities showed the convective updraft became tilted toward the rear of the system (Figure 20b). As the squall line continued to progress eastward across Lake Erie, a well defined outflow boundary became visible and pushed away from the system to the south (Figure 19d), the updraft continued to be tilted (Figure 20c), and the top of the rear-inflow appeared to descend toward to the surface (Figure 21).

The observed bow echo formation, tilted updraft, apparent sinking of the rear-inflow and presence of an outflow boundary suggest that the cold pool circulation strengthened and overwhelmed the ambient shear almost immediately upon reaching the water (RKW, Weisman 1993). Examination of the vorticity generation equation of the cold pool (right side of equation 11) suggests that the decrease in friction associated with the movement from land to water would decrease the turbulent mixing at the leading edge of the cold pool, leading to strengthening. Furthermore, observations from buoy data on Lake Erie and estimations of IBL height (Garratt, 1987) suggest that the MBL became warmer and shallower as the convection moved east. This gives evidence that the temperature gradient of the cold pool was increased, also leading to cold pool strengthening.

In addition to the observed structural changes of the squall line, the average maximum reflectivity of the storm was observed to steadily decrease, and the system's speed steadily

increased while over the water (Figure 22). While observations showed the system's updraft becoming more front-to-rear, as well as an anticipated decrease in surface-based CAPE due to the MBL, it is not clear from the available data what was the relative importance of these processes in causing the intensity to decrease. However, given evidence that the MBL actually warmed at the surface and became shallower as the convection moved east across the lake, it appears the MBL was not primarily responsible for the steady decrease. This is supported by the results of Parker (2008), who showed that squall lines maintained strong updrafts despite the increase in CIN associated with surface stable layers, given the horizontal temperature gradient that was observed in this study (≥4 K). Given this evidence, it appears the observed decrease in average maximum reflectivity was more likely due to the observed tilting of the updraft, which reduced the updraft's vertical lift leading to lower observed dBZ values.

The rapid increase in forward motion associated with the storm moving from land to water (~ 7 m s^{-1} in 15 minutes, Figure 22), as well as the rapid bow echo formation over the water, suggests the decrease in friction is the dominate mechanism which caused the cold pool's sudden increase in strength at that time. However, no observations of the frictional mixing (particularly over the lake, where variations in wind speed would cause changes in frictional mixing) were available to confirm this. While the cold pool is expected to have gotten continually stronger while moving east over the lake, the rapid speed increase, bow echo formation and updraft tilting observed in the short span of moving over the water suggests that the increase in cold pool strength due to the gradually increasing cold pool temperature gradient is not the main cause of the change in the convective structure. However, it can be speculated that it is the reason for the continued steady speed increase observed over the middle portion of

the lake. However, limitations in available observations make this difficult to confirm for this study.

The results of this case study appear to confirm the general ideas put forth in Parker (2008) and behave in agreement with the cold pool/ambient shear circulation balance proposed by RKW. However, it should be noted that the observations used in this study are not of sufficient resolution to fully confirm the relative importance of these processes. Also, it should be noted that while the general squall line behavior presented in Parker (2008) was similar to that observed in this case, the MBL in this study was of different structure (statically stable and changing depth) and considerably more shallow (max depth ~125 m) than the ~1 km deep uniform surface cool layer used his study. Further study of how squall lines react when interacting with MBLs of different depths and characteristics (including LBCs) is needed to better understand the effect of surface cool layers on mature squall lines.

References

Angevine, W. M., J. E. Hare, C. W. Fairall, D. E. Wolfe, R. J. Hill, W. A. Brewer, and A. B. White, 2006: Structure and formation of the highly stable marine boundary layer over the Gulf of Maine. *J. Geophys. Res*., **111**, D23S22.

Arritt, R. W., 1993: Effects of the large-scale flow on characteristic features of the sea breeze. *J. Appl. Meteor*., **32**, 116-125.

Augustine, J. A., and K. W. Howard, 1991: Mesoscale convective complexes over the United States during 1986 and 1987. *Mon. Wea. Rev.,* **119**, 1575-1589.

_____, W. L. Woodley, R. W. Scott and S. A. Changnon, 1994: Using geosynchronous satellite imagery to estimate summer-season rainfall over the Great Lakes. *J. Great Lakes Res.,* **20(4)**, 683-700.

Biggs, W. G. and M. E. Graves, 1962: A lake breeze index. *J. Appl. Meteor.*, **1**, 474-480.

Bluestein, H. B. and M. H. Jain, 1985: Formation of mesoscale lines of precipitation: severe squall lines in Oklahoma during the spring. *J. Atmos. Sci.*, **42**, 1711-1732.

Bryan, G. H., J. C. Knievel and M. D. Parker, 2006: A multimodel assessment of RKW theory's relevance to squall-line characteristics. *Mon. Wea. Rev*., **134**, 2772-2792.

Collins, W. G., 2001: The quality control of velocity azimuth display (VAD) winds at the National Center for Environmental Prediction. *Preprints 11th Symposium on Meteorological Observations and Instrumentation*, Amer. Meteor. Soc., Boston, MA 02108, 9.2

Coniglio, M. C. and D. J. Stensrud, 2001: Simulation of a progressive derecho using composite initial conditions. *Mon. Wea. Rev*., **129**, 1593-1616.

_____, D. J. Stensrud, and M. B. Richman, 2004: An observational study of derecho-producing convective systems. *Wea. Forecasting*, **19**, 320-337.

Doran, J. C. and S. E. Gryning, 1987: Wind and temperature structure over a land-water-land area. *J. Climate Appl. Meteor*., **26**, 973-979.

Doswell, C. A. and E. N. Rasmussen, 1994: The effect of neglecting the virtual temperature correction on CAPE calculations. *Wea. Forecasting*, **9**, 625-629.

Fankhauser, J. C., G. M. Barnes, and M. A. LeMone, 1992: Structure of a midlatitude squall line formed in strong unidirectional shear. *Mon. Wea. Rev*., **120**, 237-260.

Garratt, J. R., 1987: The stably stratified internal boundary layer for steady and diurnally varying offshore flow. *Bound.-Layer Meteor*., **38**, 369-394.

_____, 1990: The internal boundary layer- a review. *Bound.-Layer Meteor*., **50**, 171-203

Graham, R., M. Bentley, J. Sparks, B. Dukesherer, and J. Evans, 2004: Lower Michigan MCS climatology: trends, pattern types, and marine layer impacts. *Preprints 22nd Conf. on Severe Local Storms*, Amer. Meteor. Soc., Boston, MA 02108, 7B.6.

Johns, R. H., and W. D. Hirt, 1987: Derechos: widespread convectively induced windstorms. *Wea. Forecasting*, **2**, 32-49.

Klimowski, B. A., 1994: Initiation and development of rear inflow within the 28-29 June 1989 North Dakota mesoconvective system. *Mon. Wea. Rev*., **122**, 765-779.

Lafore, J.-P. and M. W. Moncrieff, 1989: A numerical investigation of the organization and interaction of the convective and stratiform regions of tropical squall lines. *J. Atmos. Sci*., **46**, 521-544.

Laing, A. G. and J. M. Fritsch, 1997: The global population of mesoscale convective complexes. *Q. J. R. Meteorol. Soc*., **123**, 389-405.

Laird, N. F., D. A. R. Kristovich, X. Liang, R. W. Arritt, and K. Labas, 2001: Lake Michigan Lake breezes, climatology, local forcing and synoptic environment. *J. Appl. Meteor.,* **40**, 409-424.

Lericos, T. P. and H. E. Fuelberg, M. L. Wiesman, and A. I. Watson, 2007: Numerical simulations of the effects of coastlines on the evolution of strong, long-lived squall lines. *Mon. Wea. Rev.*, **135**, 1710-1731.

Lyons, W. A., 1972: the climatology and prediction of the Chicago lake breeze. *J. Appl. Meteor.*, **11**, 1259-1270.

Mulhearn, P. J., 1981: On the formation of a stably stratified internal boundary layer by advection of warm air over a cooler sea. *Bound.-Layer Meteor*., **21**, 247-254.

Ogura, Y. and M-T Liou, 1980: The structure of a midlatitude squall line: a case study. *J. Atmos. Sci*., **37**, 553-567.

Parker, M. D. and R. H. Johnson, 2000: Organizational modes of midlatitude mesoscale convective systems. *Mon. Wea. Rev*., **128**, 3413-3436.

Parker, M. D., 2008: Response of simulated squall lines to low-level cooling. *J. Atmos. Sci*., **65**, 1323-1341.

Rotunno, R., J. B. Klemp, and M. L. Weisman, 1988: A theory for strong, long-lived squall lines. *J. Atmos. Sci*., **45**, 463-485.

Scott, R. W. and F. A. Huff, 1996: Impacts of the Great Lakes on regional climate conditions. *J. Great Lakes Res*., **22(4)**, 845-863.

Skyllingstad, E. D., R. M. Samelson, L. Mahrt, and P. Barbour, 2005: A numerical modeling study of warm offshore flow over cool water. *Mon. Wea. Rev*., **133**, 345-361.

Smedman, A.-S., H. Bergstroem, and B. Grisogono, 1997a: Evolution of stable internal boundary layers over a cold sea. *J. Geophys. Res*., **102**, 1091-1099.

_____, U. Hostrom, and H. Bergstroem, 1997b: The turbulence regime of a very stable marine airflow with quasi-frictional decoupling. *J. Geophys. Res*., **106**, 12437-12448.

Smull, B. F. and R. A. Houze, 1985: A midlatitude squall line with a trailing region of stratiform rain: radar and satellite observations. *Mon. Wea. Rev*., **113**, 117-133.

_____ and R. A. Houze, 1987: Rear inflow in squall lines with trailing stratiform precipitation. *Mon. Wea. Rev*., **115**, 2869-2889.

Thorpe, A. J., M. J. Miller and M. W. Moncrieff, 1982: Two-dimensional convection in non-constant shear: a model of midlatitude squall lines. *Quart. J. Roy. Meteor. Soc*., **108**, 739-762.

Wakimoto, R. W. and N. T. Atkins, 1994: Observations of the sea-breeze front during CaPE. Part I: single-doppler, satellite, and cloud photogrammetry analysis. *Mon. Wea. Rev.*, **6**, 1092-1114.

Weisman, M. L. and J. B. Klemp, 1986: Characteristics of isolated convective storms. *Mesoscale Meteorology and Forecasting*, Amer. Meteor. Soc., 331-358.

_____, J. B. Klemp and R. Rotunno, 1988: Structure and evolution of numerically simulated squall lines. *J. Atmos. Sci.*, **45**, 1990-2013.

_____, 1992: The role of convectively generated rear-inflow jets in the evolution of long- lived mesoconvective systems. *J. Atmos. Sci*., **49**, 1826-1847.

_____, 1993: The genesis of severe, long-lived bow echoes. *J. Atmos. Sci*., **50**, 645-670

_____ and R. Rotunno, 2004: "A theory for strong, long-lived squall lines" revisited. *J. Atmos. Sci*., **61**, 361-382.

Appendix A) Showing the station location (left column), station ID (middle column) and the type of data collected (right column) for each of the observation stations used in this study.

Station	ID on Figure 6	Data
Buffalo, NY	KBUF	Surface obs, RAOB, Radar, VAD
Dunkirk, NY	KDKK	Surface obs
Erie, PA	KERI	Surface obs
Ashtabula, OH	KHZY	Surface obs
Cleveland, OH	KCLE, 10	Surface obs, RAOB, Radar, Precip, VAD
Mansfield, OH	KMFD	Surface obs
Toledo, OH	KTOL	Surface obs
Ypsilanti, MI	KYPI, 3	Surface obs, Precip
Findlay, OH	KFDY	Surface obs
Defiance, OH	KDFI	Surface obs
Lambertville, MI	KDUH	Surface obs
Adrian, MI	KADG	Surface obs
Ann Arbor, MI	2	Precip
Detroit, MI (Metropolitan Airport)	KDTW, 4	Surface obs, Precip
Detroit, MI	KDTX	Surface Obs, RAOB, Radar, Precip, VAD
Windsor Riverside, ON	7	Precip
Amherstburg, MI	5	Precip
Windsor, ON	6	Precip
Kingsville, ON	8	Precip
Chatham, ON	9	Precip
Erieau, ON	CWAJ	Surface obs
NOAA Buoy 45132	45132	Surface obs
NOAA Buoy 45005	45005	Surface obs

Appendix B) Listing the year, date and time for each of the convective events used in this study, as well as the convective type. Convective types were classified as: cluster (CL), isolated (I), complex (C) and linear (L). The two columns on the far right denote the surface observations stations used to collected data upwind and downwind of Lake Erie, based on individual storm paths.

Year	Month	Day	Time Crossed Coastline (UTC)	Convective Type	Upwind Station	Downwind Station
2001	4	6	1150	CL	KDTW	KCLE
2001	5	16	1417	CL	KARB	KMFD
2001	5	26	2356	CL	KFDY	CWAJ
2001	5	26	0040	CL	KFDY	CWAJ
2001	6	15	2232	I	KFDY	KDTW
2001	6	15	2243	I	KFDY	KDTW
2001	6	20	0108	I	KDFI	CWAJ
2001	7	21	1959	C	KDTW	KCLE
2001	8	26	2022	I	KYIP	KERI
2001	9	7	2302	I	KFDY	KDTW
2001	9	7	2314	I	KFDY	KDTW
2001	9	24	0033	L	KDFI	CWAJ
2001	10	25	0046	L	KADG	KERI
2002	4	13	0044	CL	KADG	KCLE
2002	4	19	0827	L	KADG	KCLE
2002	6	5	1406	C	KTOL	CWAJ
2002	6	5	1319	C	KTOL	CWAJ
2002	6	21	2004	C	KDTW	KERI
2002	7	21	1844	L	KDTW	KMFD
2002	7	22	1634	C	KADG	CWAJ
2002	7	26	1535	I	KTTF	CWAJ
2002	7	28	0328	C	KTOL	CWAJ
2002	7	28	0159	I	CWAJ	KERI
2002	7	29	2359	L	KTOL	KCLE
2002	7	29	2146	C	KADG	KCLE
2002	8	4	2310	I	KADG	KCLE
2002	8	14	1917	CL	KFDY	CWAJ
2002	9	20	1705	I	KMFD	CWAJ
2002	9	20	1901	I	KMFD	CWAJ
2002	9	20	1832	I	KMFD	CWAJ
2002	12	18	0300	CL	KTOL	CWAJ
2003	4	30	1706	L	KADG	KERI
2003	5	1	0159	L	KADG	KERI
2003	5	11	1111	CL	KFDY	CWAJ
2003	6	8	1614	L	KFDY	KERI
2003	6	19	556	CL	CWAJ	KERI
2003	7	6	2011	I	KADG	KMFD
2003	7	8	1913	I	KDTW	KCLE

2003	7	21	0721	CL	KADG	KCLE
2003	8	15	1238	CL	KDTW	KCLE
2003	8	16	2003	CL	KDTW	KCLE
2003	8	22	0328	C	KDTW	KCLE
2003	9	27	0348	L	KDUH	KERI
2004	5	9	2221	CL	KTTF	KCLE
2004	5	9	0637	I	KTTF	CWAJ
2004	5	21	0357	C	KTOL	CWAJ
2004	5	10	2247	CL	KTOL	CWAJ
2004	5	17	1851	CL	KDTW	KCLE
2004	6	17	2113	L	KTTF	KCLE
2004	7	14	0604	L	CWAJ	KERI
2004	7	31	0004	CL	KCLE	CWAJ
2004	8	3	0602	L	KDTW	KCLE
2004	8	27	1734	L	KTOL	CWAJ
2005	5	13	2040	I	KTOL	CWAJ
2005	6	9	2000	I	KTOL	CWAJ
2005	6	9	0001	CL	KCLE	CWAJ
2005	6	28	0116	CL	CWAJ	KCLE
2005	6	30	1608	L	KTTF	KCLE
2005	7	18	2241	L	KTTF	KCLE
2005	7	21	0457	C	KTTF	KCLE
2005	7	26	1842	L	KDTW	KERI
2005	8	20	1313	C	KCLE	CWAJ
2005	8	13	2321	CL	KTTF	KCLE
2006	1	13	1415	C	KCLE	CWAJ
2006	2	4	1603	L	KCLE	CWAJ
2006	4	1	0102	L	KDTW	KCLE
2006	4	12	2028	L	KDTW	KCLE
2006	5	14	2027	CL	KCLE	CWAJ
2006	5	25	2027	L	KTOL	CWAJ
2006	5	31	2034	CL	KTTF	KCLE
2006	6	8	2120	CL	KDTW	KCLE
2006	6	19	1808	L	KTTF	KCLE
2006	7	14	2023	L	KTTF	KCLE
2006	7	27	0104	C	KDTW	KERI
2006	7	30	2059	L	KDTW	KERI
2006	8	3	1152	C	KTTF	KCLE
2006	9	13	2047	I	KCLE	KDTW
2006	9	12	0403	CL	KCLE	CWAJ
2007	3	1	1247	C	KCLE	CWAJ
2007	3	27	2138	L	KDTW	KTOL
2007	5	1	1958	L	CWAJ	KERI
2007	5	15	2312	C	KTOL	CWAJ

Appendix B) continued.

2007	6	3	1501	C	KCLE	KTTF
2007	7	5	2022	I	KDTW	KCLE
2007	7	27	0548	CL	KDTW	KCLE
2007	8	6	0707	I	CWAJ	KEIR
2007	8	9	0634	L	KTTF	KERI
2007	8	23	1144	L	KDTW	KERI
2007	8	24	0427	C	KTTF	KCLE

Appendix B) continued.

Appendix C) Listing the definitions (far right) and abbreviations (middle) of each of the parameters (left) created for analysis in this study.

Parameter	Abbreviation	Definition
Time Moved Over Water	TMOW	Time, both in UTC and LST, of radar scan when the geographical center of convection moved over lakeshore.
Starting dBZ	Start dBZ	The maximum base reflectivity of the convection 30 minutes prior to TMOW. In cases where convection did not exist 30 minutes prior, this variable is the first radar scan with maximum reflectivity > 35 dBZ.
Time Moved Over Water dBZ	TMOW dBZ	The maximum base reflectivity of the convection at the time it moved over the coastline.
End dBZ	End dBZ	The maximum base reflectivity at the last radar scan that the storm was monitored, either due to the reflectivity dropping below 45dBZ or the storm moving over the downwind shore.
30min dBZ	+30min dBZ	The maximum base reflectivity of the convection at the time scan closest to 30 minutes after it had moved over the lake.
60min dBZ	+60min dBZ	The maximum base reflectivity of the convection at the time scan closest to 60 minutes since it had moved over the lake.
90min dBZ	+90 min dBZ	The maximum base reflectivity of the convection at the time scan closest to 90 minutes since it had moved over the lake.
Delta dBZ	ΔdBZ	The total change in maximum base reflectivity experienced by the convection over the lake, taken as the difference of the last measured reflectivity and the TMOW reflectivity.
Delta 30min dBZ	Δ30min dBZ	Change in max reflectivity 30 minutes after the stormed crossed the lakeshore: 30min dBZ – TMOW dBZ.
Delta 60min dBZ	Δ60min dBZ	Change in max reflectivity 60 minutes after the stormed crossed the lakeshore: 60min dBZ – TMOW dBZ. Cases where the convection died or moved over the downwind shore are not included.
Delta 90min dBZ	Δ90min dBZ	Change in max reflectivity 90 minutes after the stormed crossed the lakeshore: 90min dBZ – TMOW dBZ. Cases where the convection died or moved over the downwind shore are not included.
Delta 30-60min dBZ	Δ30-60min dBZ	Change in max reflectivity in the time period of 30-60 minutes after the storms crossed the lakeshore. 60min dBZ – 30min dBZ.
Delta 60-90min dBZ	Δ60-90min dBZ	Change in max reflectivity in the time period of 60-90 minutes after the storms crossed the lakeshore. 90min dBZ – 60min dBZ.

Appendix C) continued.

Upwind Temperature	UWT (t)	Upwind temperature as measured from the surface observation station nearest the convective path before the convection moved over the lake. Data were collected from at least -4 to +2 hours of time convection crossed the lakeshore.
Upwind Wind Speed	UWspd (t)	Upwind wind speed as measured from the surface observation station nearest the convective path before the convection moved over the lake. Data were collected from at least -4 to +2 hours of time convection crossed the lakeshore.
Upwind Wind Direction	UWdir (t)	Upwind wind direction as measured from the surface observation station nearest the convective path before the convection moved over the lake. Data were collected from at least -4 to +2 hours of time convection crossed the lakeshore.
Downwind Temperature	DWT (t)	Downwind temperature as measured from the surface observation station nearest the convective path as the convection moved over the lake. Data were collected from at least -2 to +5 hours of time convection crossed the lakeshore.
Downwind Wind Speed	DWspd (t)	Downwind wind speed as measured from the surface observation station nearest the convective path as the convection moved over the lake. Data were collected from -2 to +5 hours of time convection crossed the lakeshore.
Downwind Wind Direction	DWdir (t)	Downwind wind direction as measured from the surface observation station nearest the convective path as the convection moved over the lake. Data were collected from -2 to +5 hours of time convection crossed the lakeshore.
Lake Temperature	LT (t)	Temperature of Lake Erie taken from buoy 45005, when available. Data were collected from -4 to +4 hours of the time convection crossed the lakeshore.
Lake Air Temperature	LAT (t)	Temperature of air above Lake Erie taken from buoy 4505, when available. Data were collected from -4 to +4 hours of the time convection crossed the lakeshore.
Cold Pool Temperature	CPT	Temperature of the convection's cold pool, as determined from upwind surface temperature observations at the time nearest convective passage. Hourly temperature data from upwind observation sites were analyzed subjectively for clear evidence of a cold pool; any cooling that was deemed due to diurnal cooling or frontal passages was rejected.

Appendix C) continued.

Cold Pool Strength	CP	The temperature anomaly due to the presence of the cold pool, calculated as the difference in temperature of the cold pool and environment before the cold pool.
Temperature Difference LT-LAT	LT-LAT	The difference in temperature between the water temperature and air temperature over the lake, taken at the hour closest to the convection moving over water.
Temperature Difference LAT-UWT	LAT-UWT	The difference in temperature between the air temperature over the lake (from the hour closest to the convection moving over water) and the ambient upwind temperature over land (pre-cold pool).
Temperature Difference CP-LAT	CP-LAT	The difference in temperature between the cold pool and the air temperature over the lake, using the lake air temperature from the hour closest to the convection moving over water.
Temperature Difference UWT-DWT	UWT-DWT	The difference in temperature between the upwind and downwind temperatures, using the upwind temperature from the hour before convective passage over the observation site and the temperature from the hour closest to the convection reaching the downwind observation site. In cases where the convection did not reach the downwind shore, the temperature from the hour closest to the convection moving over the water is used.
2.5 km Shear	2.5 km Shear	The wind speed recorded from corresponding RAOB nearest 2.5 km.
6 km Shear	6 km Shear	The wind speed recorded from corresponding RAOB nearest 6 km.

Appendix C) continued.

Tables and Figures

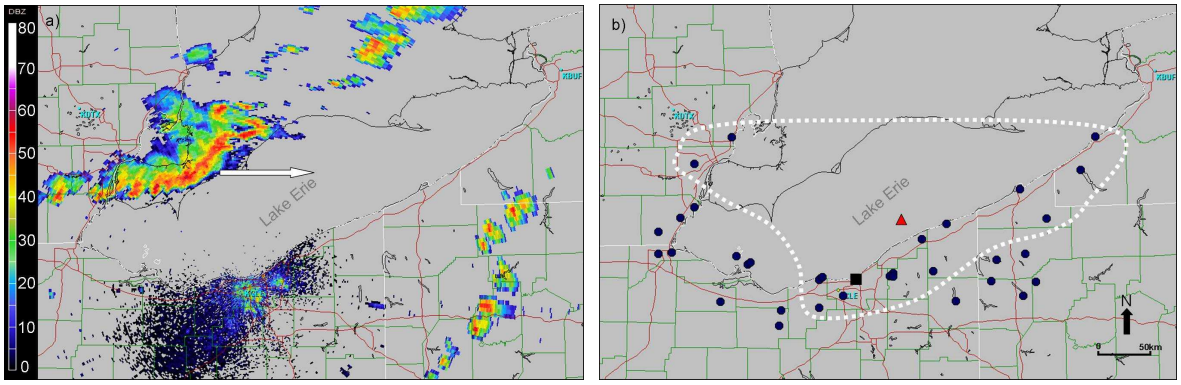

Figure 1) Base reflectivity from KCLE at 1822 UTC (a) and storm reports from the Storm Predication Center (b) for 26 July 2005. White arrow in (a) denotes direction of squall line motion. The locations of high wind reports in (b) are denoted by circles, severe wind reports (>34 m s^{-1}) denoted by squares, and a severe wind report (~50 m s^{-1}) from a ship on Lake Erie is denoted by a triangle. The dotted line in (b) denotes storm reports corresponding to the original squall line as determined from squall line evolution as depicted in radar data.

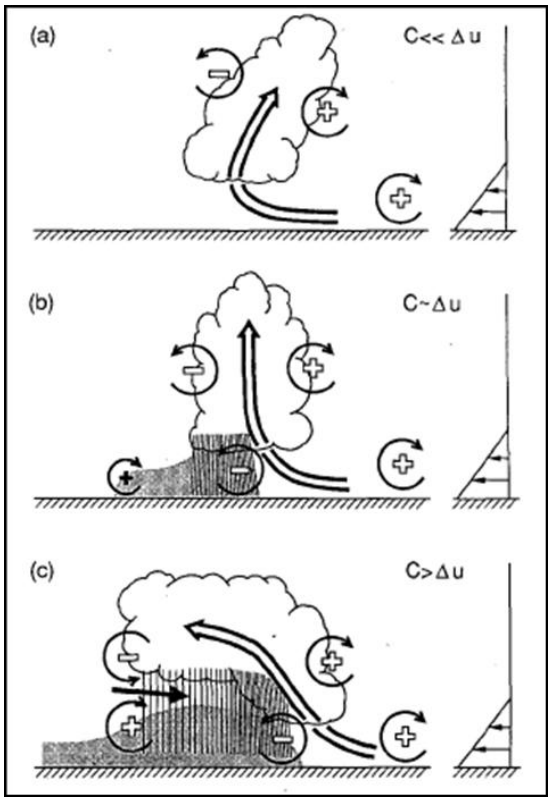

Figure 2) Three stages of squall line life cycle: (a) updraft tilts downshear, (b) erect updraft and maximum intensity and (c) updraft tilts upshear and systems begins to weaken. *C* represents buoyancy parameter of the cold pool, *ΔU* represents ambient storm-relative wind shear (from Weisman 1992).

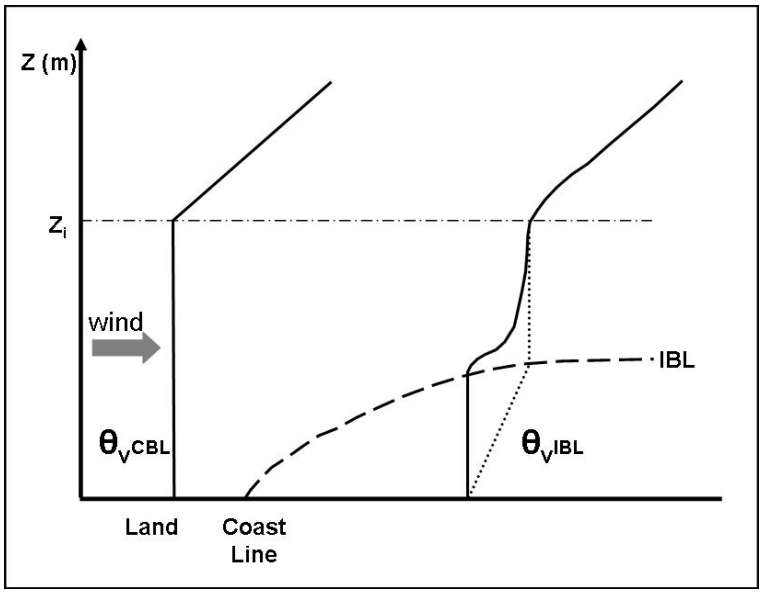

Figure 3) Conceptual model of IBL formation, adapted from Smedman et al. (1997a). Z_i denotes height of the convective boundary layer top over land. Gray arrow denotes wind direction, solid black lines denote virtual potential temperature profiles, and dotted black line denotes temperature profile in instances of a stable IBL.

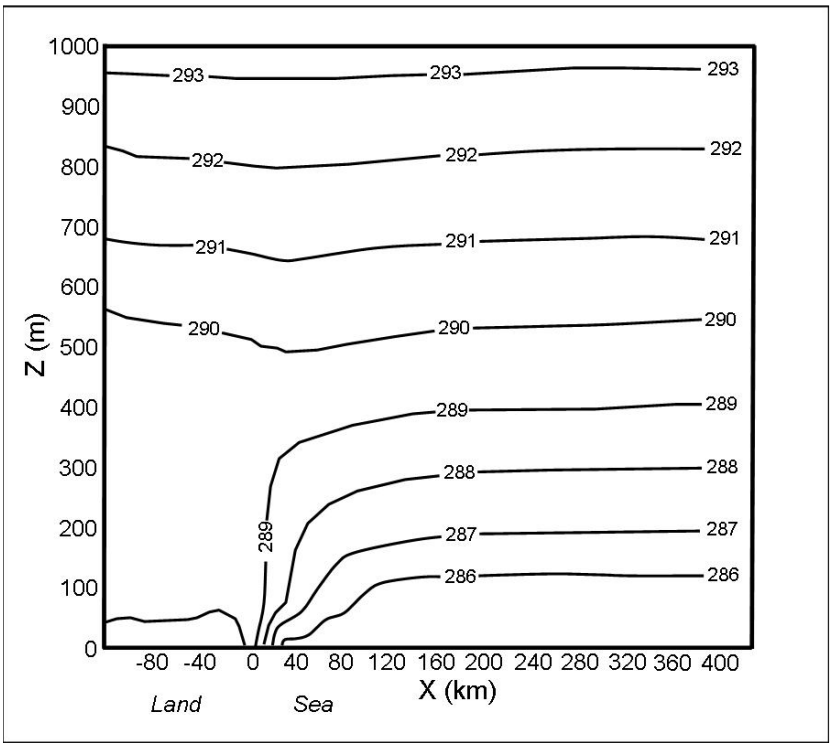

Figure 4) From Smedman et al. (1997a) showing simulated potential temperature (Kelvin) as a function of height (Z) and distance from the shoreline (X). Simulation shows results for a land that is 6 K warmer than the water surface and a synoptic wind (left to right) of 5 m s^{-1}.

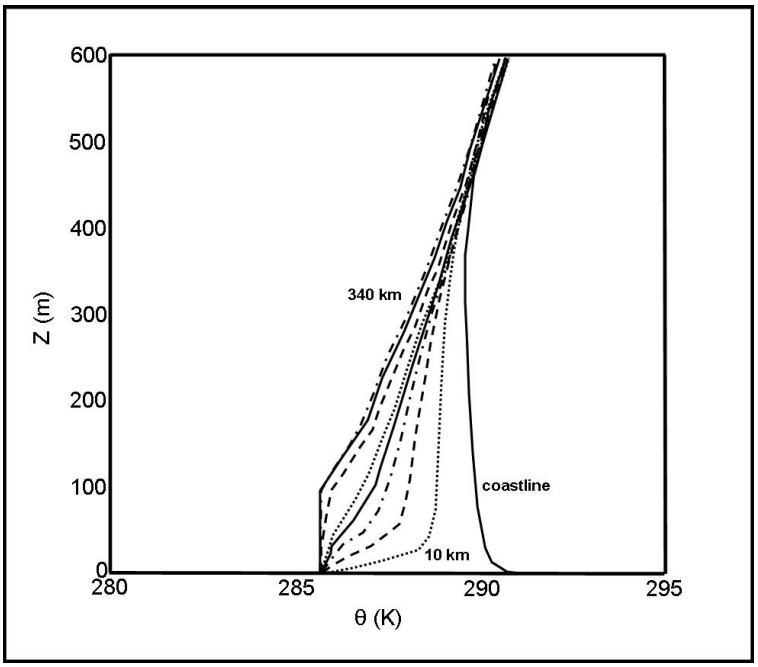

Figure 5) From Smedman et al. (1997a) showing a simulation of potential temperature (Kelvin) as a function of height for varying distances from the coastline for a land/water temperature difference of 6 K and synoptic wind of 5 m s^{-1}.

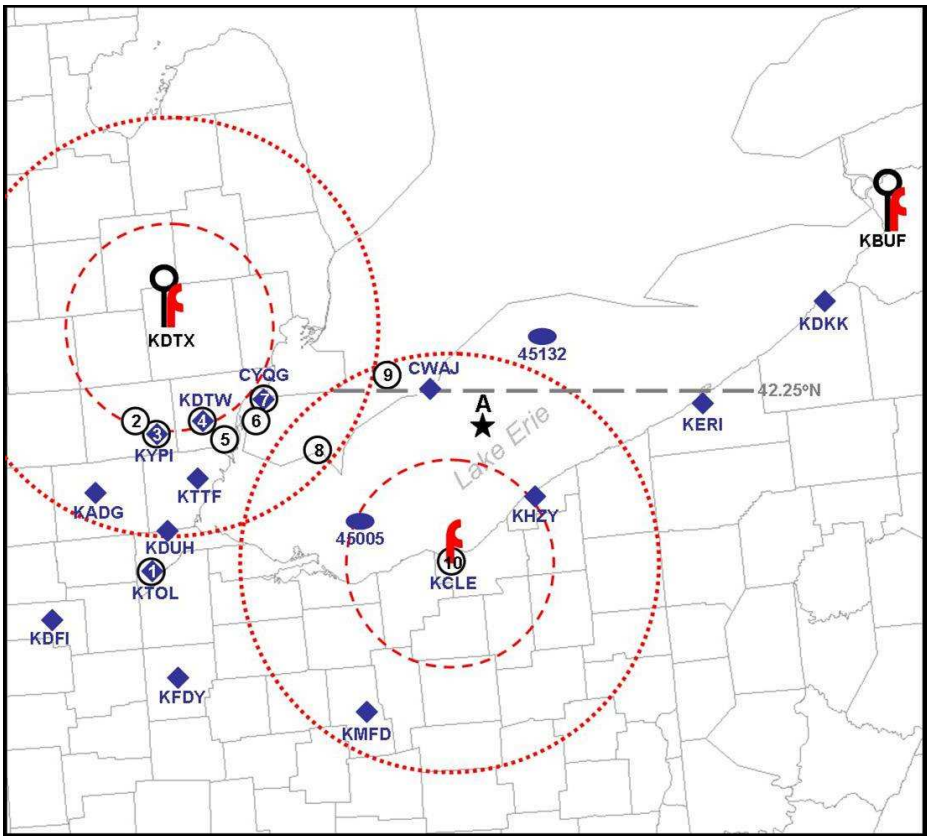

Figure 6) Location of observation sites used in this study. Surface observation sites denoted by blue diamonds, precipitation observation sites denoted by numbered black circles, buoys denoted by blue ovals, radar locations denoted by , and RAOB sounding sites by . Radar range for KCLE and KDTX denoted by red dashed circle (50 km) and red dotted circle (100 km). Black star located over Lake Erie denotes location of GFS40 created soundings. Gray dashed line denotes 42.25°N, the northern boundary of the climatological study. Names and locations of precipitation sites in Appendix A.

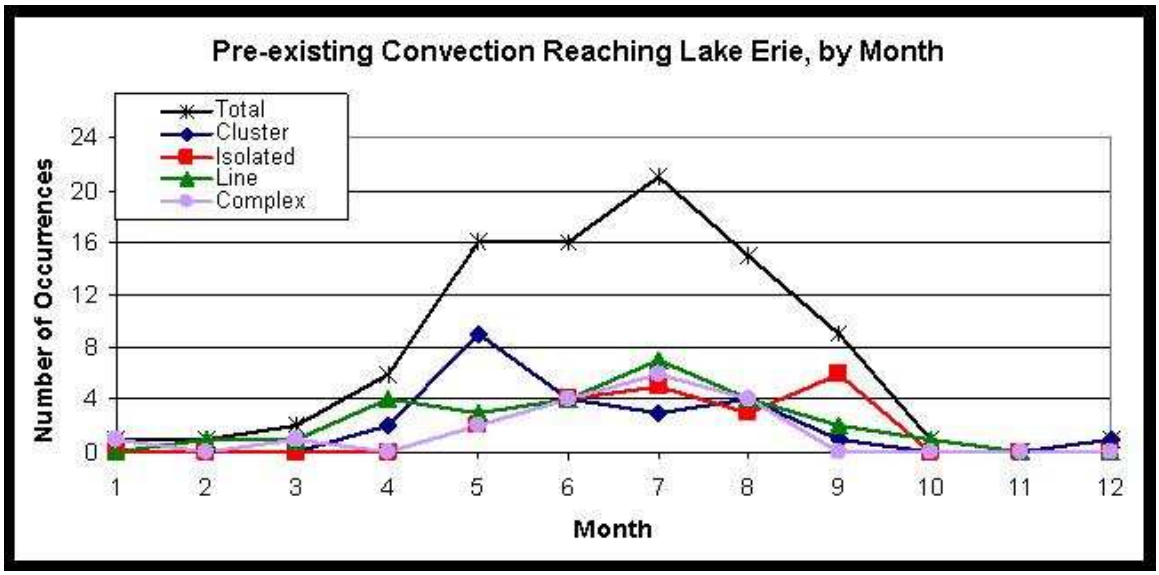

Figure 7) Number of occurrences (89 total) of each convective type by month.

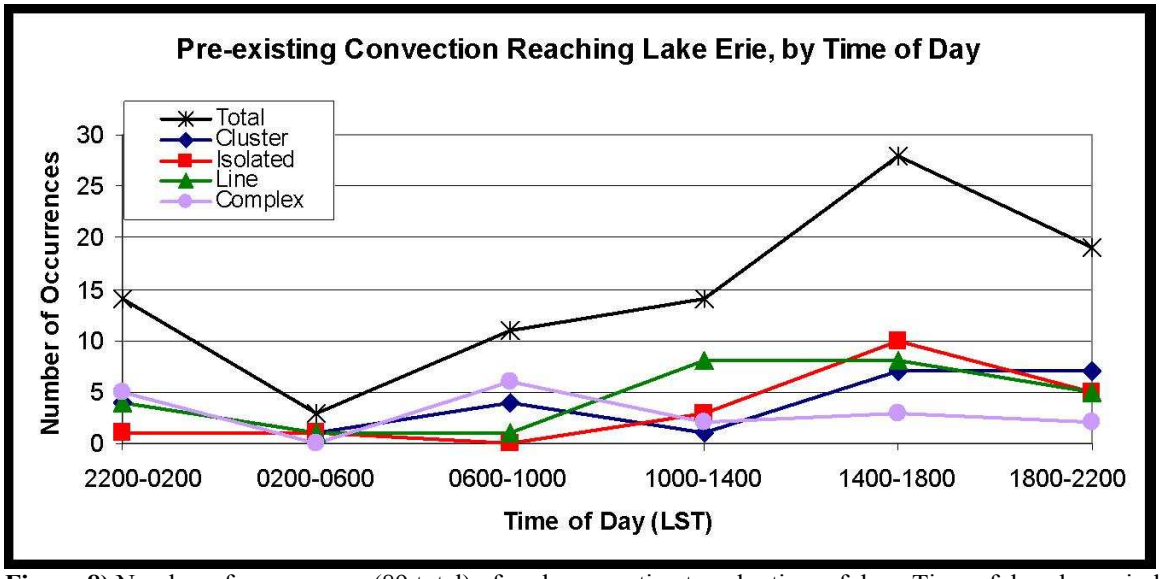

Figure 8) Number of occurrences (89 total) of each convective type by time of day. Time of day shown in local standard time (LST=UTC – 5 hr).

+30 Mins

	> +8 dBZ	+3/+7 dBZ	+2/-2 dBZ	-3/-7 dBZ	< -8 dBZ	Died	Onshore
Total	00	07	55	29	08	01	00
Cluster	00	04	63	25	08	00	00
Isolated	00	05	45	40	05	05	00
Linear	00	07	59	26	07	00	00
Complex	00	11	50	28	11	00	00

+60 Mins

	> +8 dBZ	+3/+7 dBZ	+2/-2 dBZ	-3/-7 dBZ	< -8 dBZ	Died	Onshore
Total	00	04	37	20	11	18	09
Cluster	00	04	25	21	13	25	13
Isolated	00	00	25	15	15	35	10
Linear	00	07	48	22	07	07	07
Complex	00	06	50	22	11	06	06

Table 1) Percentage of events of each convective type (rows) that experienced associated changes in maximum reflectivity (columns) at 30 minutes (top) and 60 minutes (bottom) over water. Column titled "died" denotes percentage of events which maximum reflectivity fell below 45 dBZ, column titled 'onshore' denotes percentage of events which moved over land on downwind shore.

+30 Mins

	Avg ΔdBZ	St Dev
Total	-1.82	3.78
Cluster	-1.92	3.61
Isolated	-2.37	4.62
Linear	-1.41	3.37
Complex	-1.72	3.88

+60 Mins

	Avg ΔdBZ	St Dev
Total	-2.60	4.60
Cluster	-4.33	5.51
Isolated	-3.73	4.41
Linear	-1.57	3.64
Complex	-1.69	3.79

Table 2) Average maximum reflectivity change and standard deviation of maximum reflectivity change of convective events at 30 minutes (top) and 60 minutes (bottom) over water.

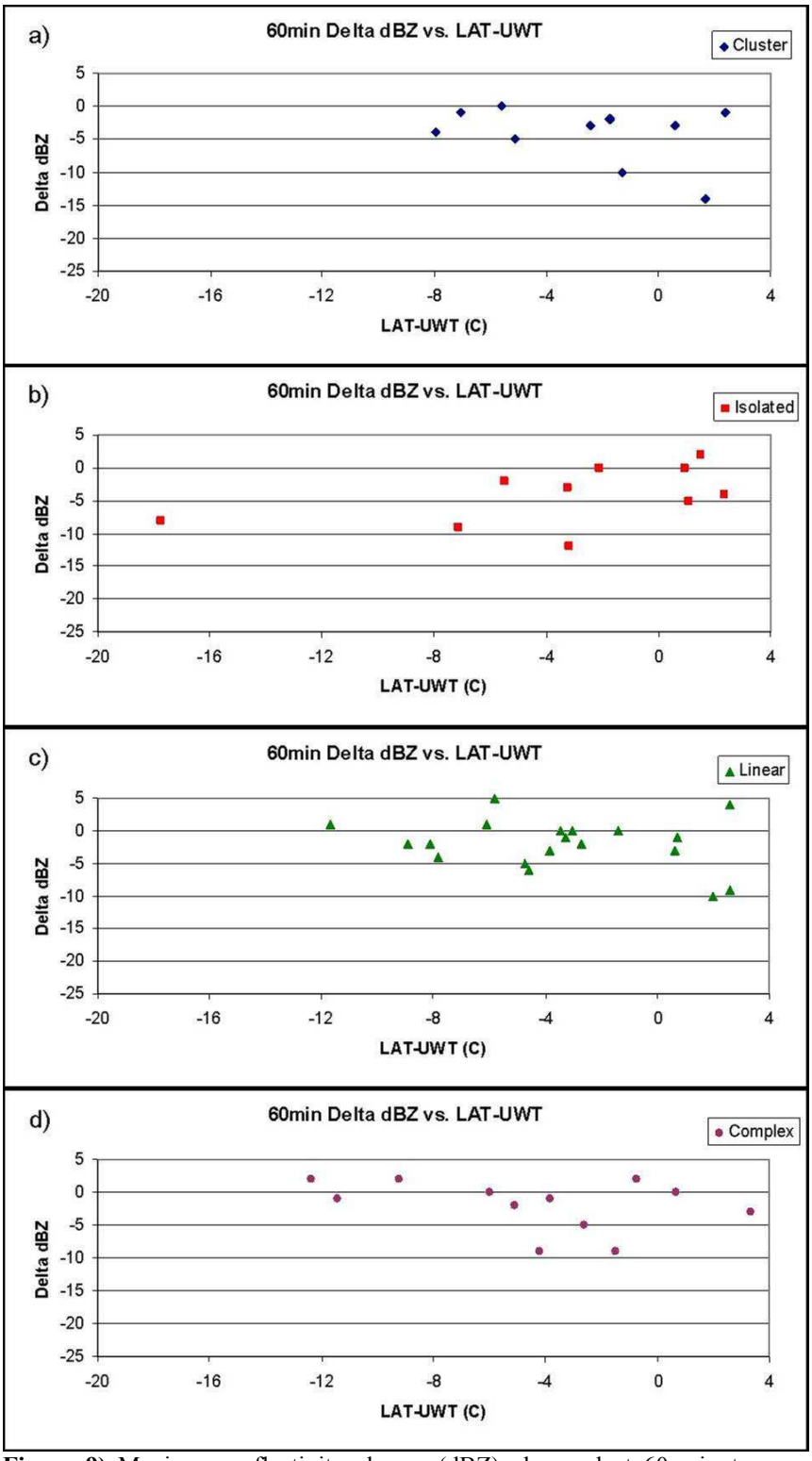

Figure 9) Maximum reflectivity change (dBZ) observed at 60 minutes over Lake Erie versus the temperature difference (^{o}C) between the over-lake and upwind land air temperature (LAT-UWT).

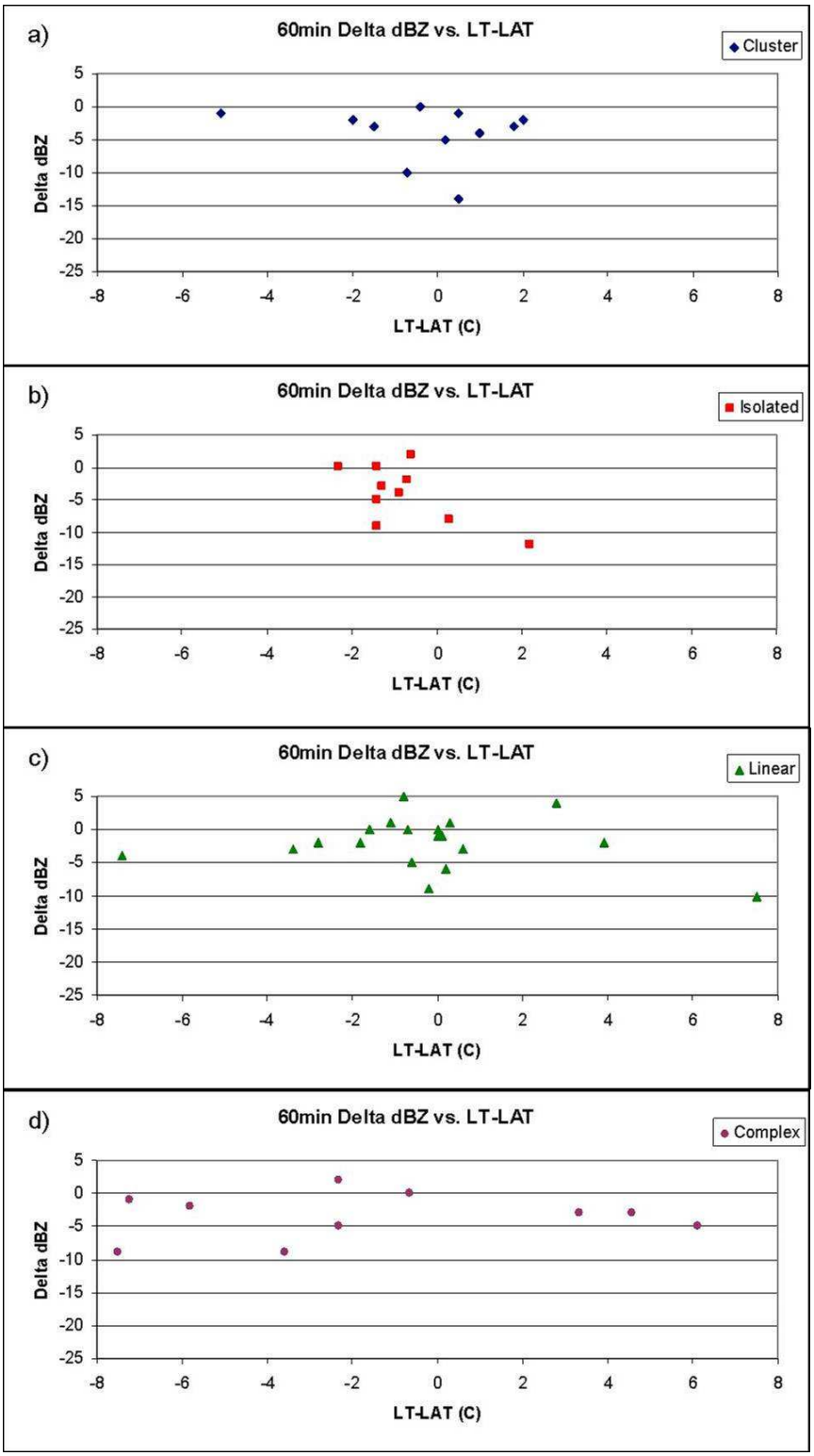

Figure 10) Maximum reflectivity change (dBZ) observed at 60 minutes over Lake Erie versus the temperature difference (^{o}C) between the lake surface water temperature and over-lake air temperature (LT-LAT).

+60 min	LAT	LAT-UWT	LT-LAT	DWT-UWT	CPT-LAT	3 km Shear	#	# CP
Total	00	-.13	-.21	-.08	.34	.06	62	21
Cluster	.32	-.35	-.19	-.08	.31	-.22	15	5
Isolated	.43	.49	***-.65***	.30	--	.19	11	3
Linear	-.14	-.27	-.17	-.02	.47	-.15 **(.53)**	23	9
Complex	-.29	-.39	-.16	-.16	.18	.05	16	4

Table 3) Showing correlation values between maximum reflectivity change at +60 minutes over Lake Erie and selected atmospheric parameters (columns) for each of the convective types (rows). Column titled '#' denotes number of events for each convective type for the LAT, LAT-UWT, LT-LAT and UWT-DWT variables. Column titled '# CP' denotes number of events for each convective type for which the CPT-LAT variable was available. Correlation values of statistical significance for α=.05 are shaded and bolded; correlations were not conducted for samples sizes 3 or less. Number in parenthesis for linear, 3 km shear is the correlation value between maximum reflectivity change +60 mins and 3 km shear values <15 m s^{-1}. Reference Appendix C for description of how each variable was defined.

a) LAT-UWT Positive

+60 min	LAT	LAT-UWT	LT-LAT	DWT-UWT	CPT-LAT	#	# CP
Total	.14	-.03	-.29	-.01	--	16	2
Cluster	--	--	--	--	--	3	0
Isolated	-.71	-.23	.48	-.42	--	4	0
Linear	.05	-.14	.05	.42	--	5	1
Complex	.35	**-.94**	**-.99**	**-.99**	--	4	1

b) LAT-UWT Negative

+60 min	LAT	LAT-UWT	LT-LAT	DWT-UWT	CPT-LAT	#	# CP
Total	-.02	-.01	-.15	.19	-.06	38	22
Cluster	.53	-.41	-.18	-.23	.28	8	5
Isolated	.45	**.95**	-.78	.15	--	6	3
Linear	-.23	-.18	.20	.14	.43	14	9
Complex	-.31	**-.67**	-.06	.22	.11	10	5

c) LT-LAT Positive

+60 min	LAT	LAT-UWT	LT-LAT	UWT-DWT	CPT-LAT	#	# CP
Total	.07	.05	-.21	.10	-.24	21	7
Cluster	.25	-.16	.40	-.38	--	6	2
Isolated	--	--	--	--	--	2	1
Linear	.03	-.14	-.52	.01	--	9	3
Complex	**.99**	.48	-.68	**-.97**	--	4	1

d) LT-LAT Negative

+60 min	LAT	LAT-UWT	LT-LAT	UWT-DWT	CPT-LAT	#	# CP
Total	-.14	-.25	00	.20	.30	33	16
Cluster	.54	-.52	-.35	-.18	--	5	3
Isolated	-.39	.48	.08	-.05	--	8	1
Linear	-.32	-.50	.14	.37	.49	10	7
Complex	-.24	-.32	.10	.25	.02	10	5

Table 4) Showing correlation values between maximum reflectivity change at 60 minutes over Lake Erie and select atmospheric parameters (columns) for each of the convective types (rows). Each table shows correlations of atmospheric variables for cases where LAT-UWT was positive (a) and negative (b) and LT-LAT was positive (c) and negative (d). Column titled '#' denotes number of events for each convective type for the LAT, LAT-UWT, LT-LAT and UWT-DWT variables. Colum titled '# CP' denotes number of events for each convective type for which the CPT-LAT variable was available. Correlation values of statistical significance for α=.05 are shaded and bolded; correlations were not conducted for samples sizes 3 or less. Reference Appendix C for description of how each variable was defined.

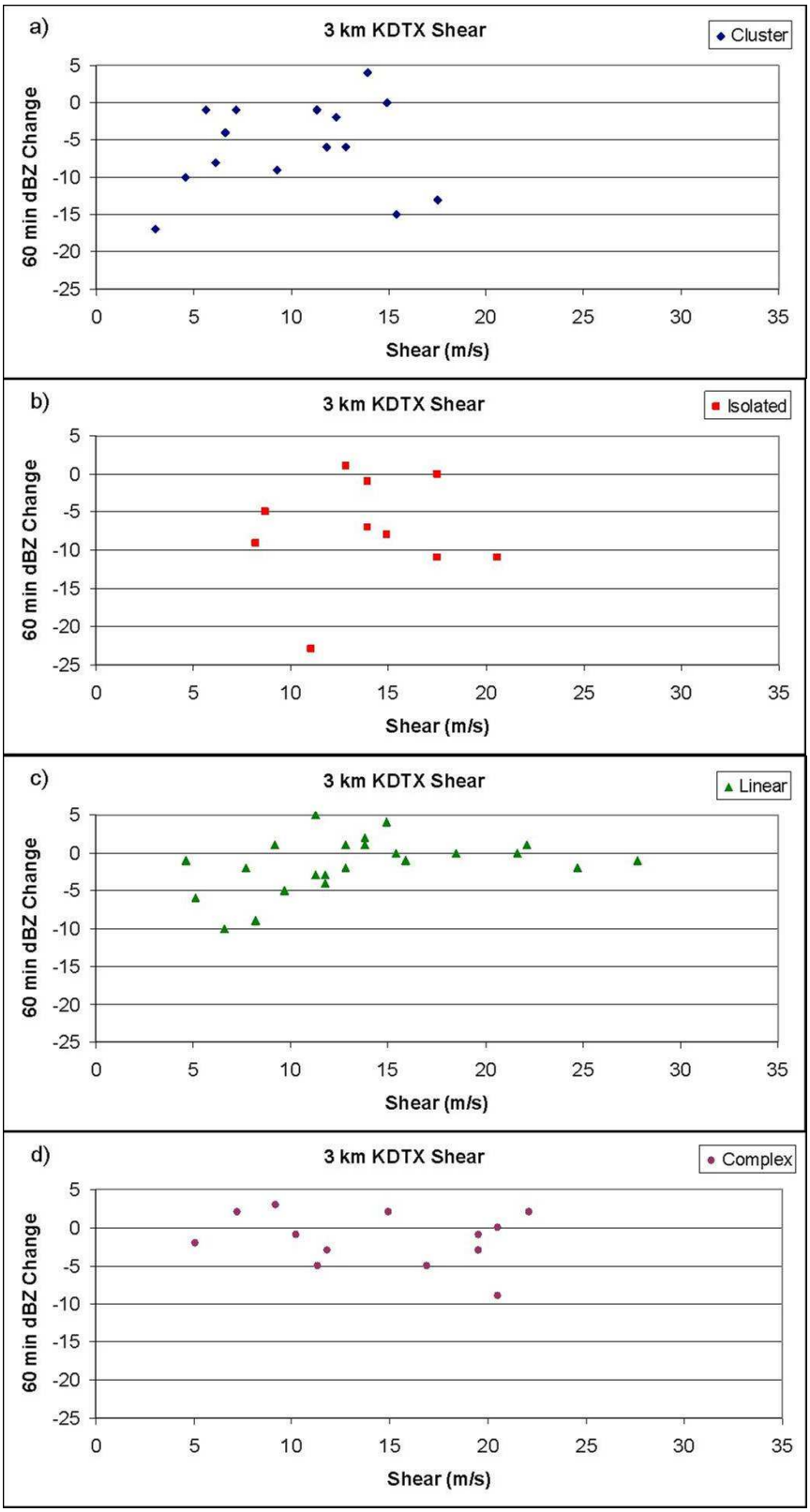

Figure 11) Maximum reflectivity change (dBZ) observed at 60 minutes over Lake Erie versus the surface-3 km vertical wind shear (m s^{-1}) observed at KDTX for the four convective types.

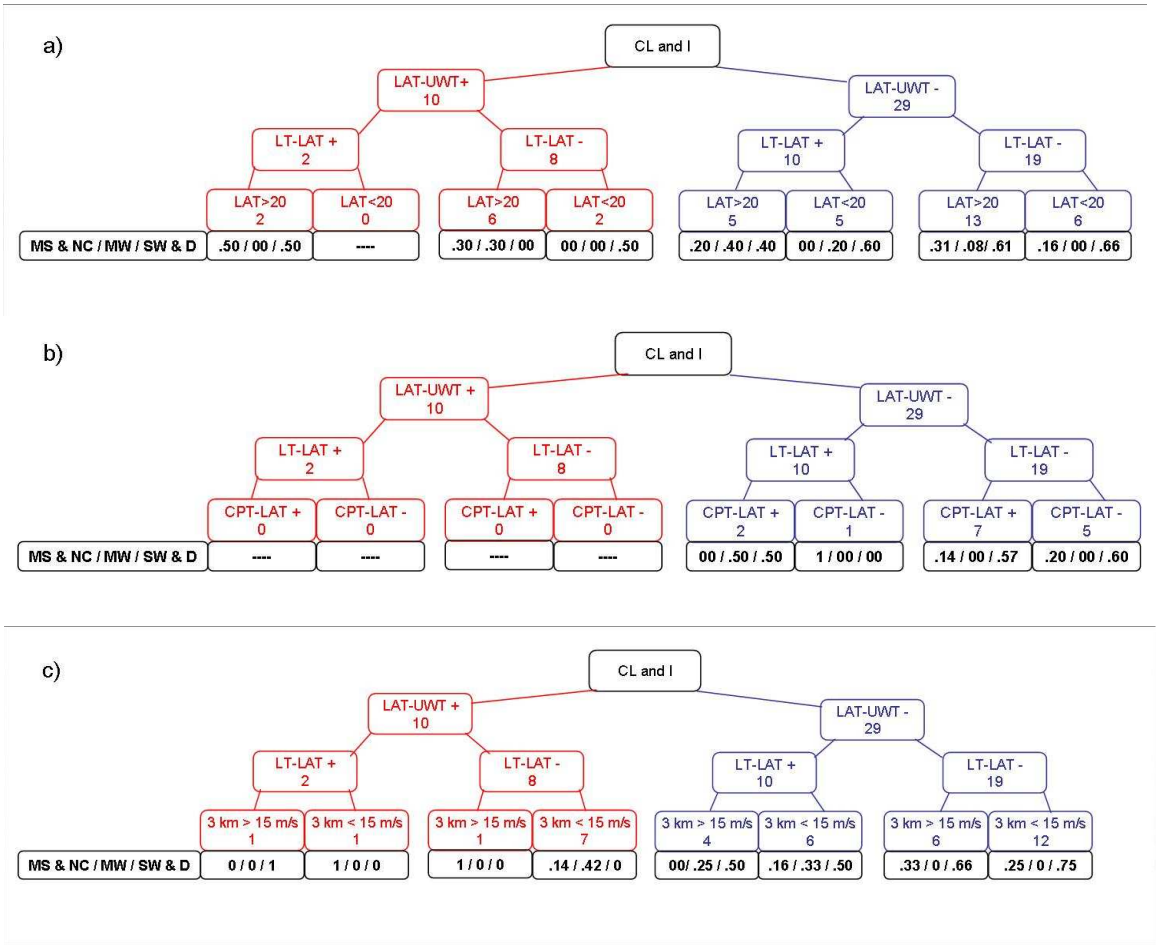

Figure 12) Flowcharts for cluster and isolated convective systems. Numbers displayed in rows 2 thru 4 show number of convective events which occurred under the corresponding environmental conditions. Row 5 (black) denotes fraction of storms which experienced corresponding changes in reflectivity as defined at far left of row 5: moderately strengthened (MS) and no change (NC) / moderately weakened (MW) / significantly weakened (SW) and died (D).

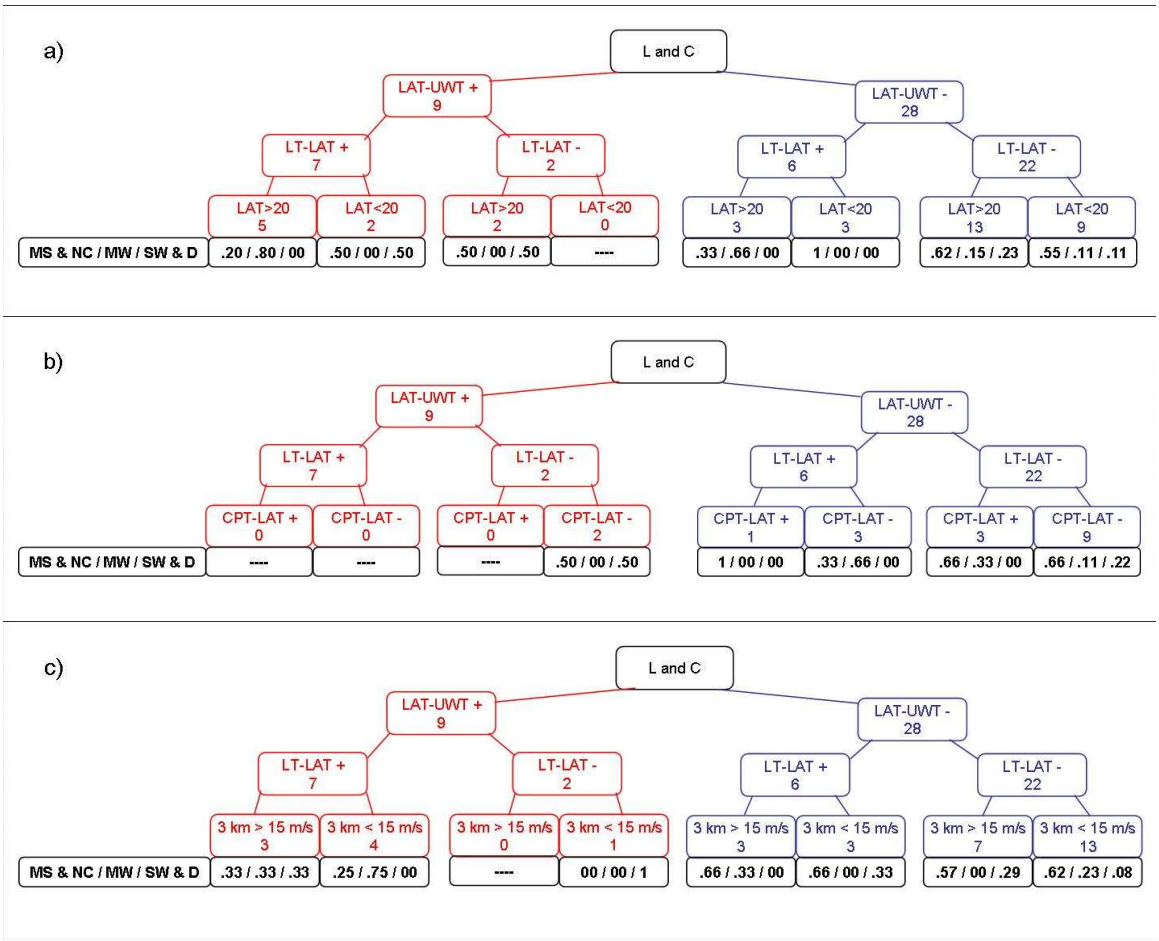

Figure 13) Flowcharts for linear and complex convective systems. Numbers displayed in rows 2 thru 4 show number of convective events which occurred under the corresponding environmental conditions. Row 5 (black) denotes fraction of storms which experienced corresponding changes in reflectivity as defined at far left of row 5: moderately strengthened (MS) and no change (NC) / moderately weakened (MW) / significantly weakened (SW) and died (D).

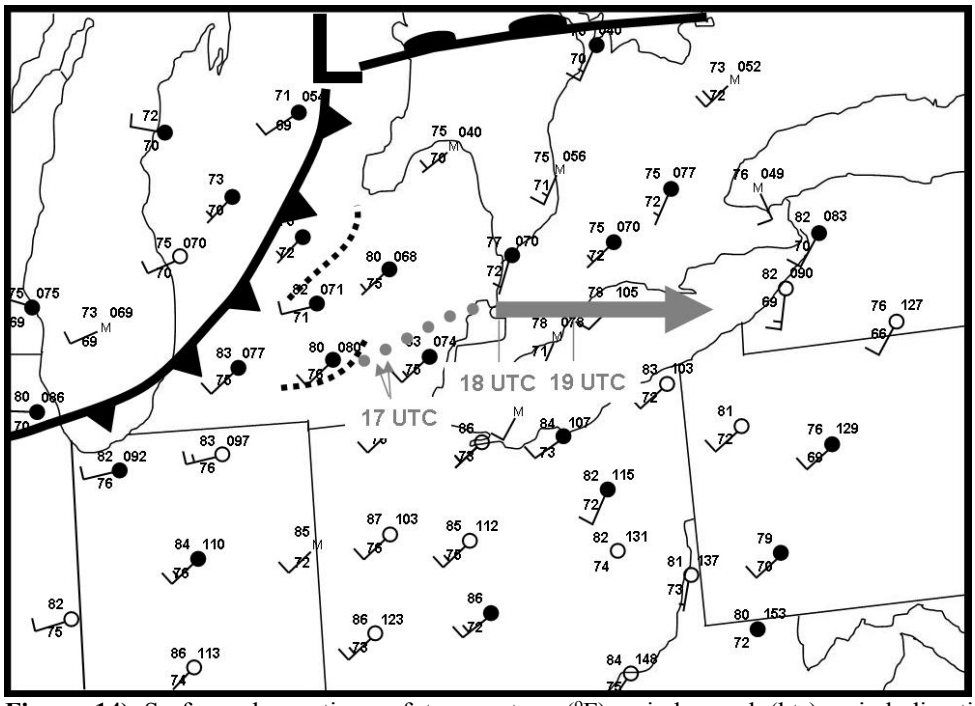

Figure 14) Surface observations of temperature (°F), wind speed (kts), wind direction and frontal boundary locations from the NCDC at 1500 UTC. Dotted lines in lower Michigan represent locations of pre-existing outflow boundaries. Path of convection from 1700-1900 UTC denoted by large dotted gray line (when convection was organized as individual cells) and thick gray arrow (when convection was organized as squall line).

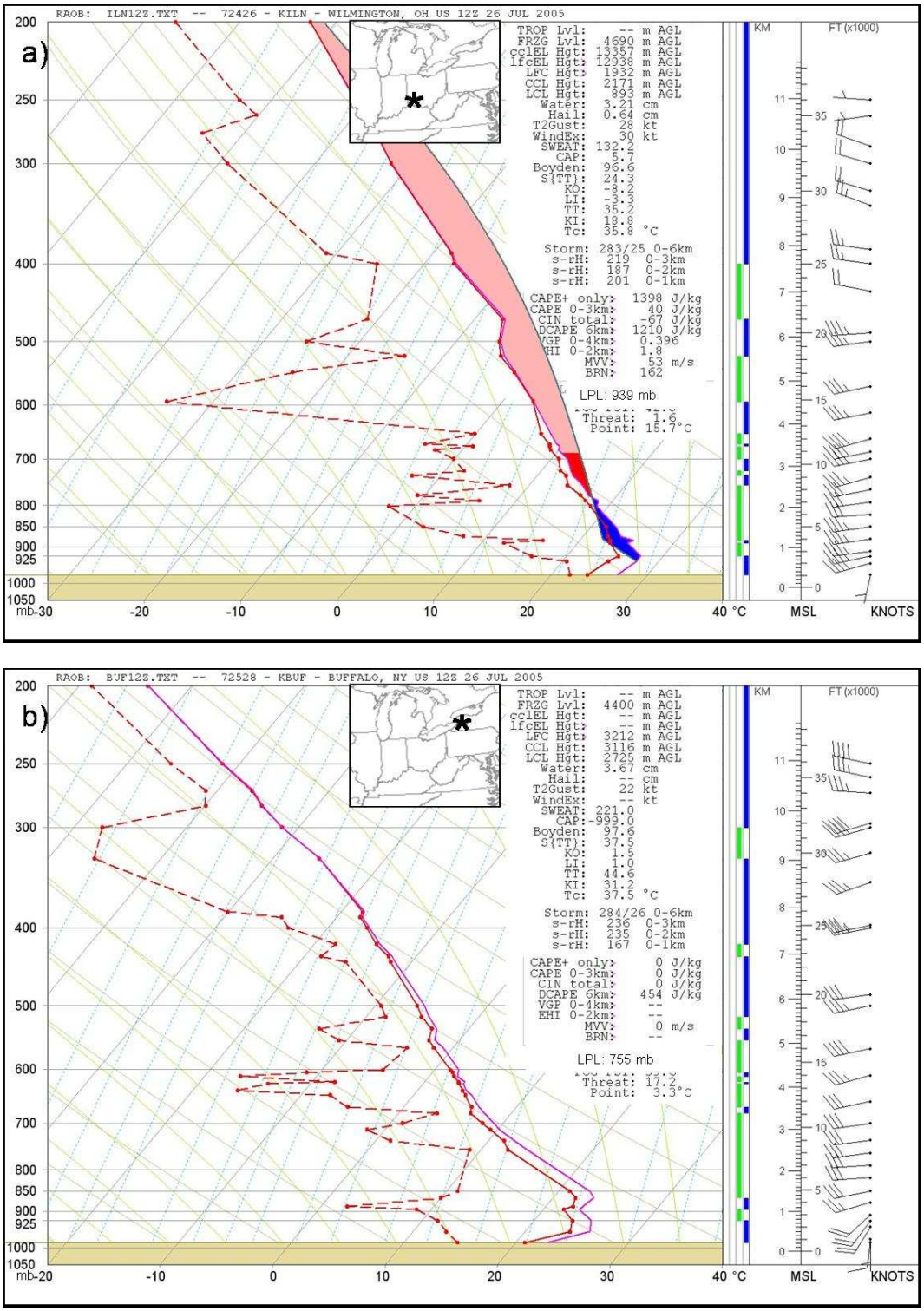

Figure 15) Skew-T RAOB soundings from 12 UTC July 26, 2005 from (a) Wilmington, OH b)Buffalo, and c) Detroit, MI. Red dashed line denotes dewpoint temperature, red solid line denotes temperature, and pink solid line denotes virtual temperature. Convective inhibition (CIN, J kg^{-1}) shaded in blue, CAPE (J kg^{-1}) shaded in pink. CAPE shown is 300 hPa most unstable CAPE (MUCAPE), determined from the most unstable parcel in the lowest 300 hPa, and is calculated using virtual temperature (Doswell and Rasmussen 1994). Lifted Parcel Level (LPL) denotes most unstable parcel. Location of RAOB site denoted at top middle inset.

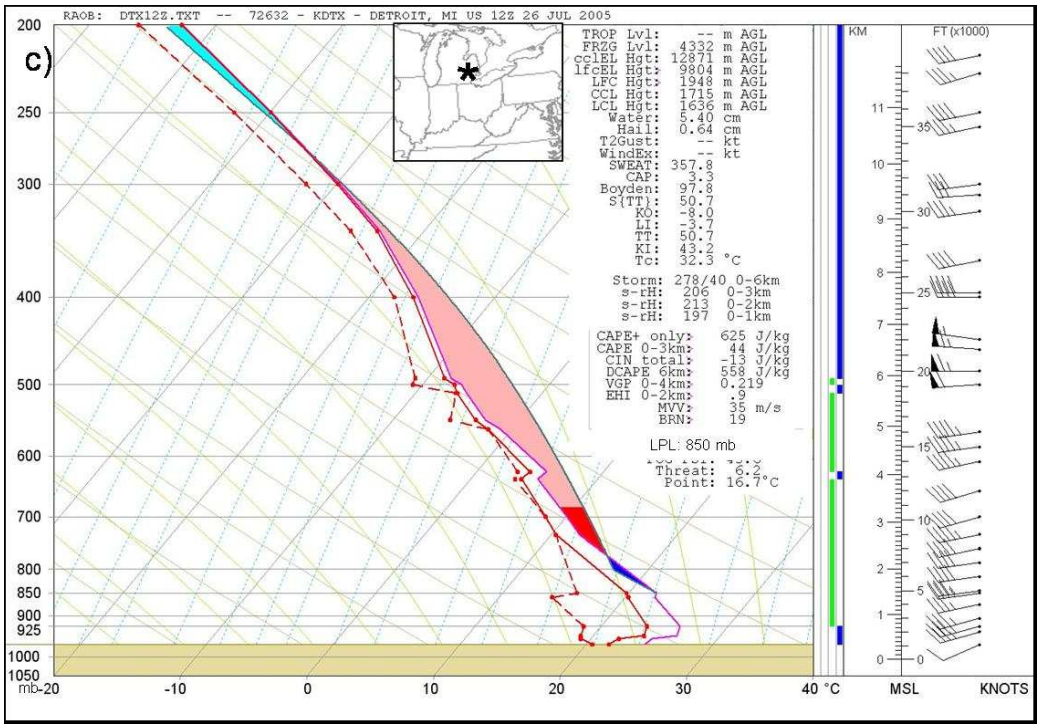

Figure 15) continued.

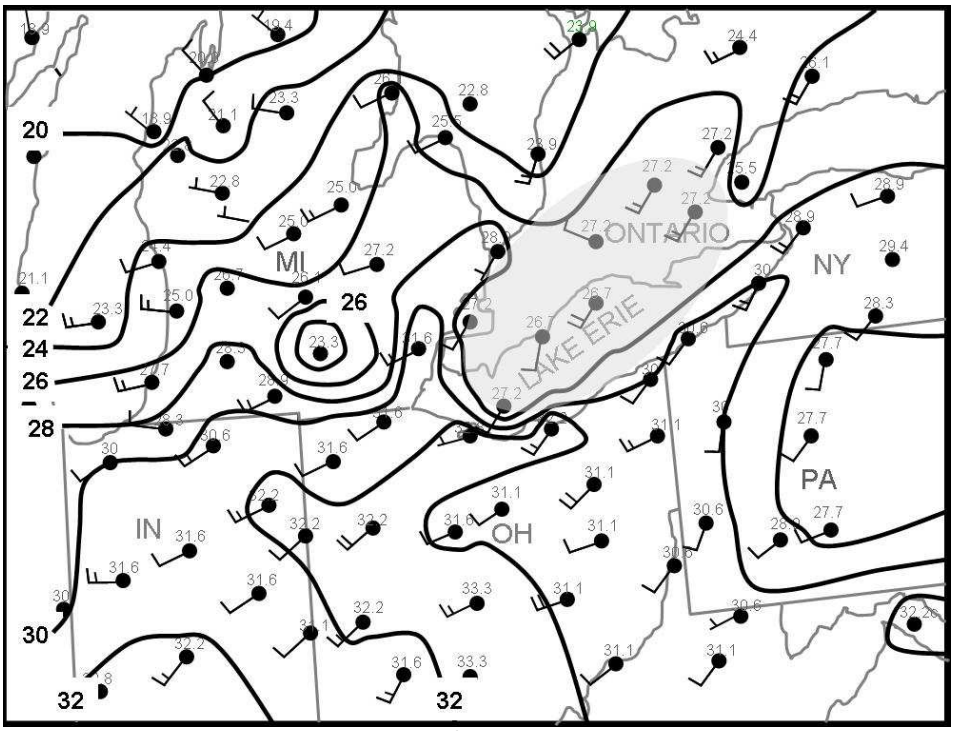

Figure 16) Plot of surface temperature (°C), surface wind speed (kts) and direction from surface observations at 1700 UTC, isotherms drawn every 2°C. Gray shading denotes lake-cooled air (MBL). Closed isotherms in southern Michigan denote location of forming surface cold pool due to developing convection.

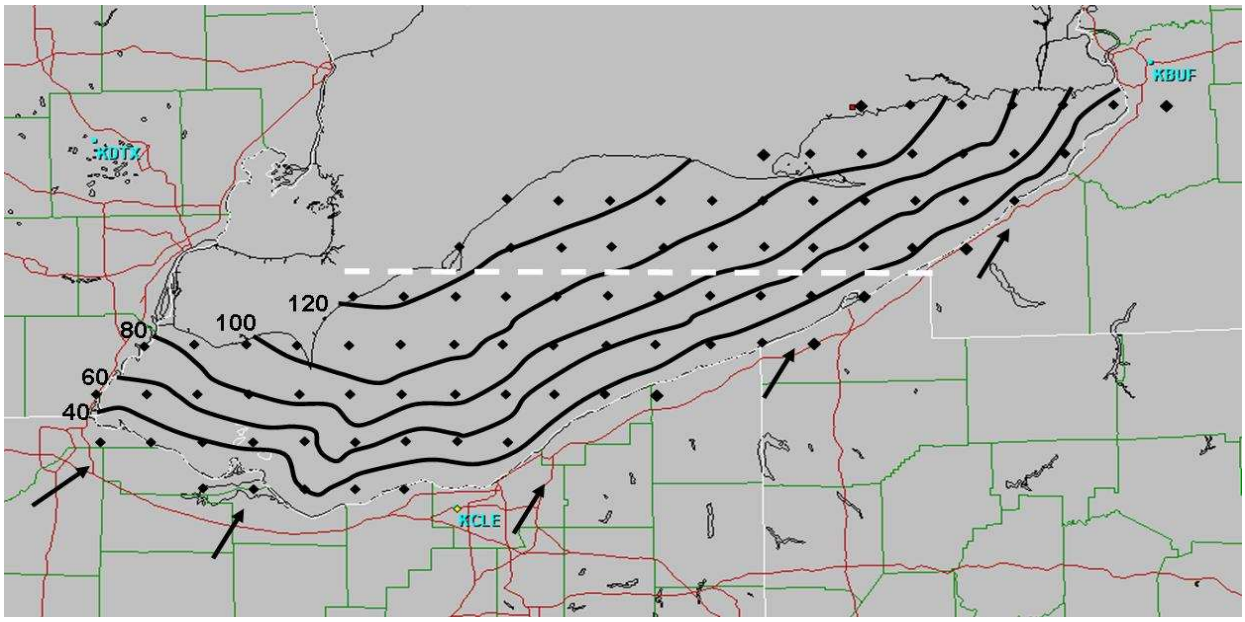

Figure 17) Showing grid constructed over Lake Erie (black diamonds) and estimated IBL depth (black lines) in meters. Grid points were placed 18 km due east (90^{o}) and north (360^{o}) of preceding point. Black arrows denote average surface wind direction. White dashed line denotes location of conceptual diagram displayed in Figures 3 and 12.

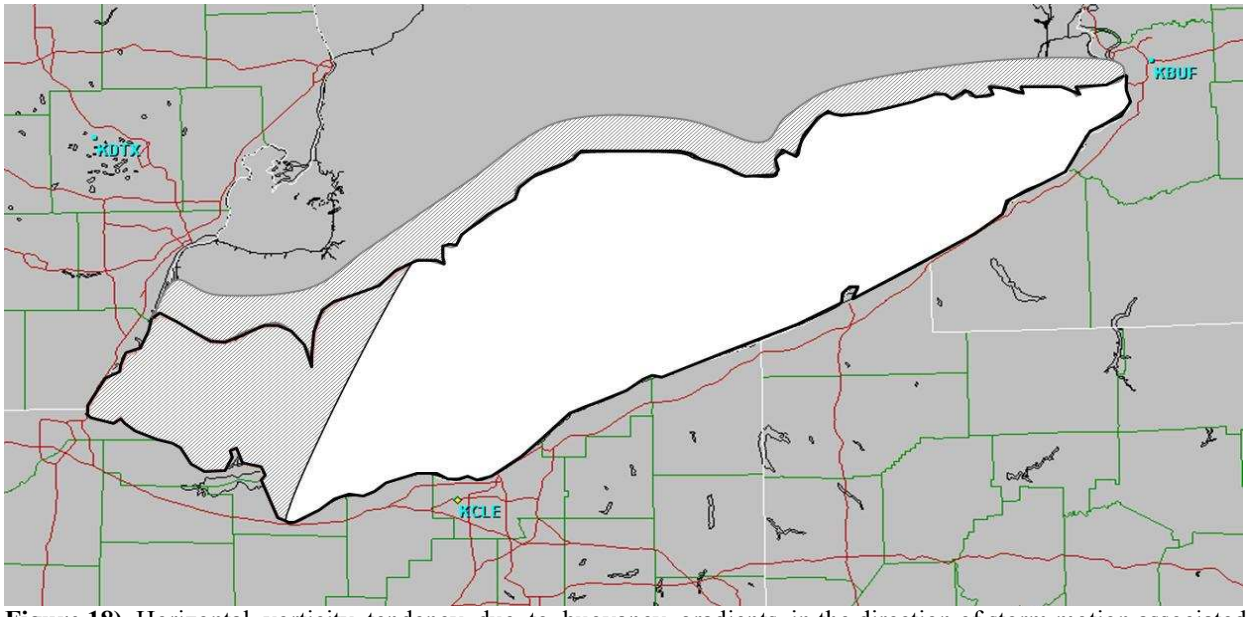

Figure 18) Horizontal vorticity tendency due to buoyancy gradients in the direction of storm motion associated with the presence of the IBL over Lake Erie. Light gray shading denotes positive vorticity tendency, white shading denotes negative vorticity tendency

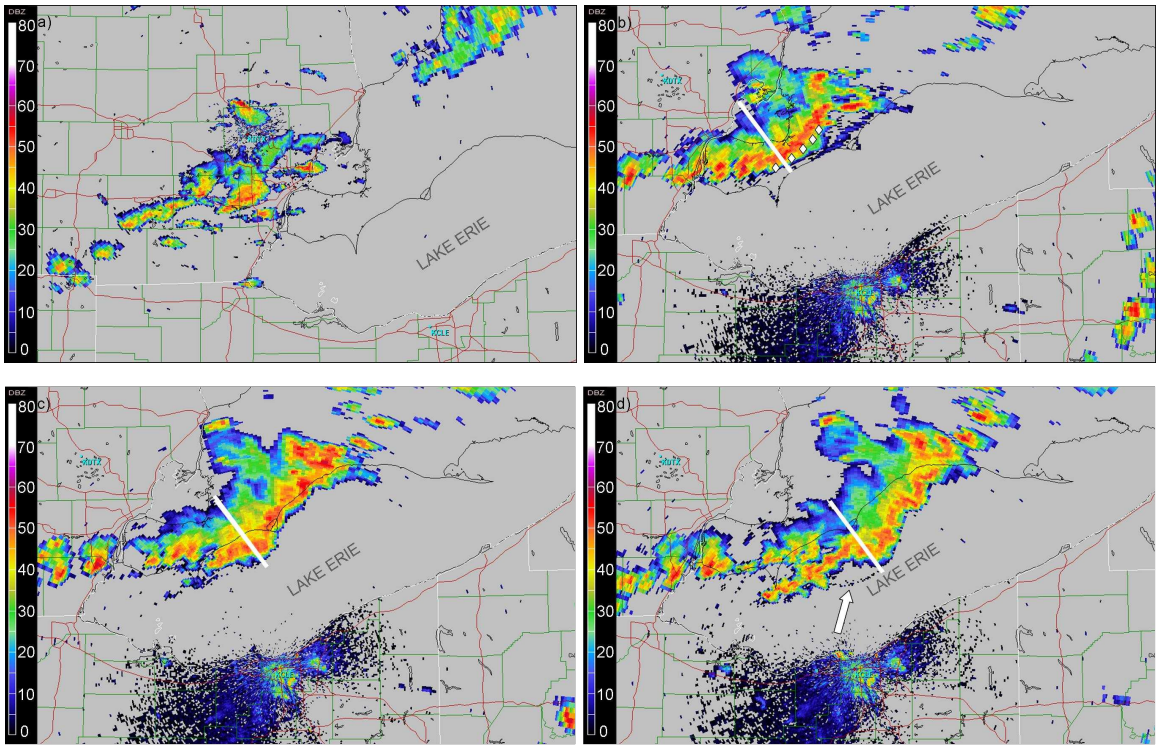

Figure 19) Showing radar reflectivity (a-d) from 26 July 2005. Base reflectivity from a) KDTX at 1717 UTC, b) KCLE at 1822 UTC, c) KCLE at 1853 UTC and d) KCLE at 1913 UTC. The white lines on panels (b), (c) and (d) denote locations of SRV cross sections in Figure 20, which are constant in position relative to the squall line. White diamonds in panel b) show latitudes where average storm velocity and base reflectivity were measured. White arrow in panel d) denotes location of outflow boundary.

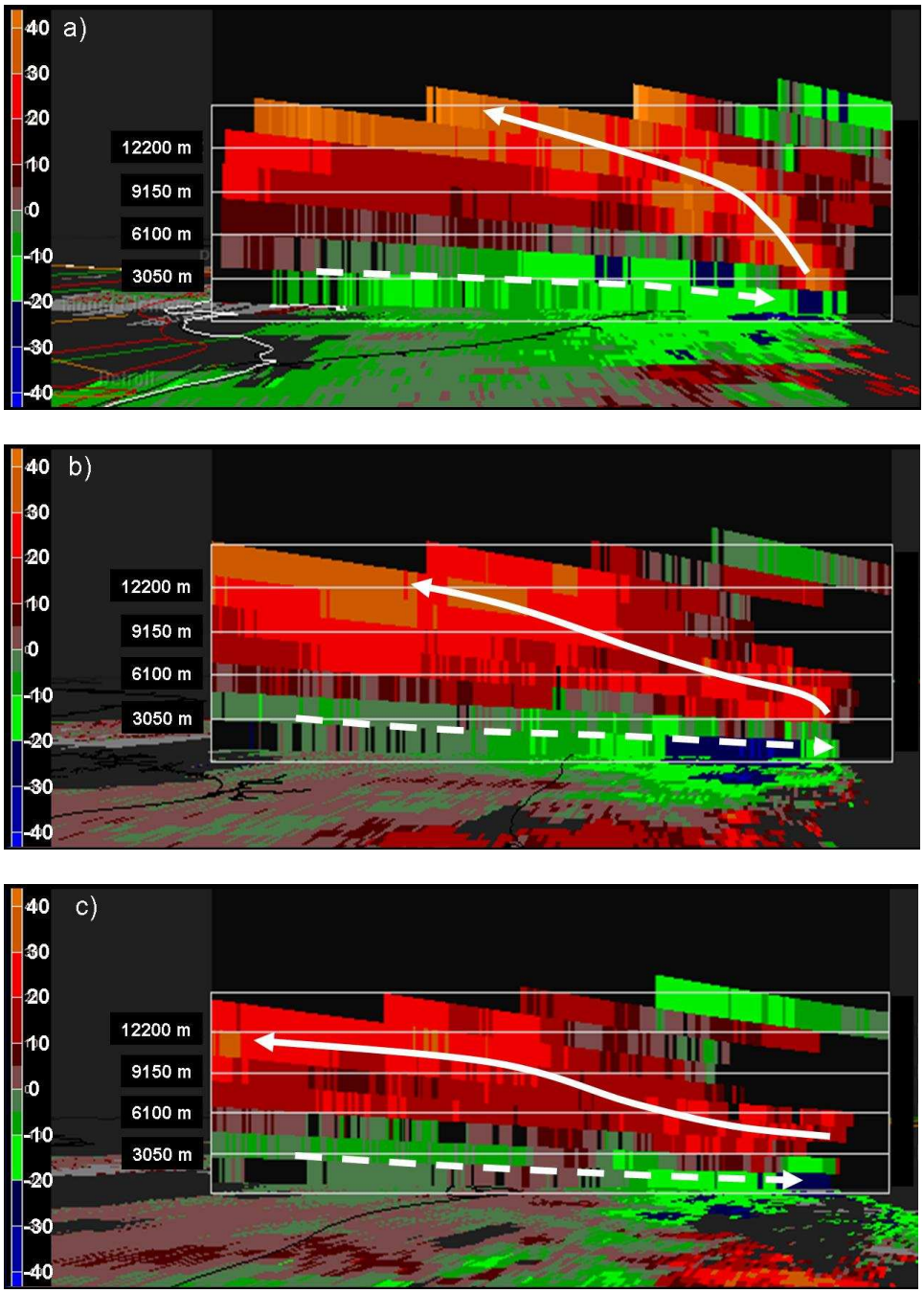

Figure 20) Storm relative velocity (SRV) cross-sections from KCLE at a) 1822 UTC, b) 1853 UTC and c) 1913 UTC. Red/orange shading denotes positive SRV (m s^{-1}) values (away from radar), green/blue shading denotes negative values (toward radar). Refer to Figure 19b-d for locations of cross-sections relative to the squall line.

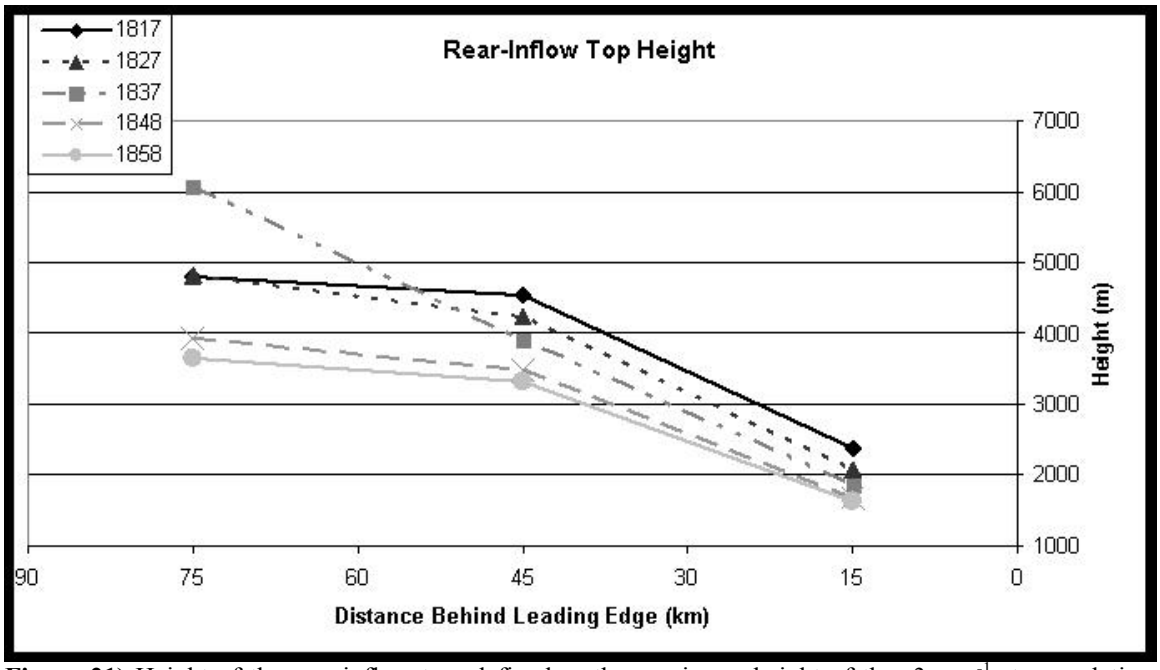

Figure 21) Height of the rear-inflow top, defined as the maximum height of the -3 m s^{-1} storm-relative velocity. Height was determined at 15 km, 45 km and 75 km behind the leading edge of the convective line.

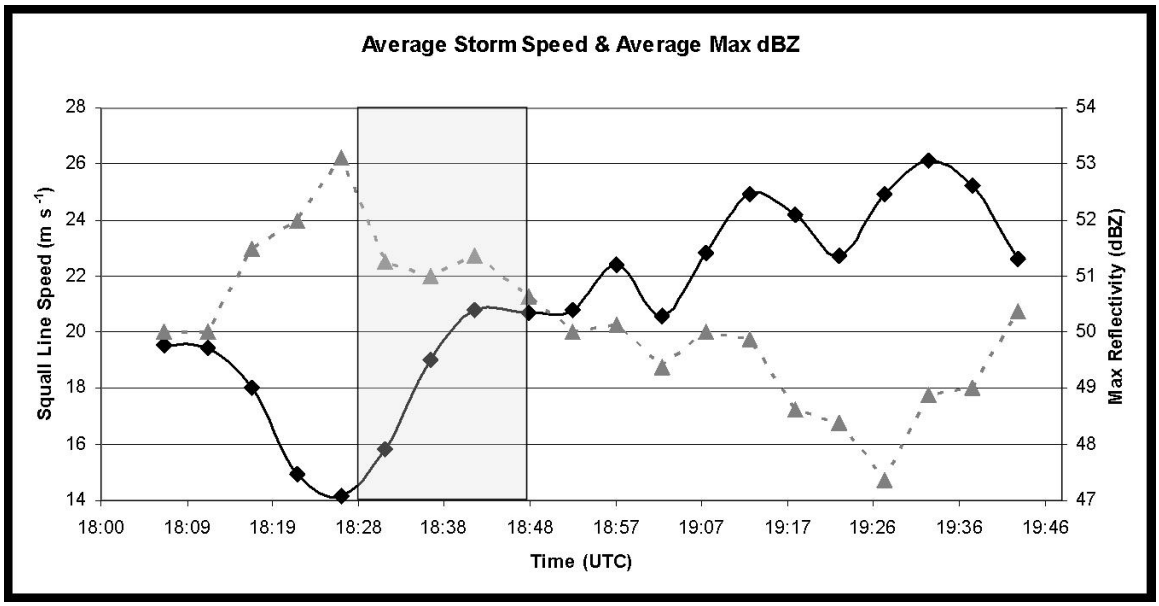

Figure 22) Average storm motion (denoted by solid black line) and average max base reflectivity (denoted by gray dotted line) of the squall line from 1807 – 1943 UTC. Gray shaded area shows time convection moved from land to water. Average storm motion and reflectivities determined from the 5 latitude points in Figure 19b.

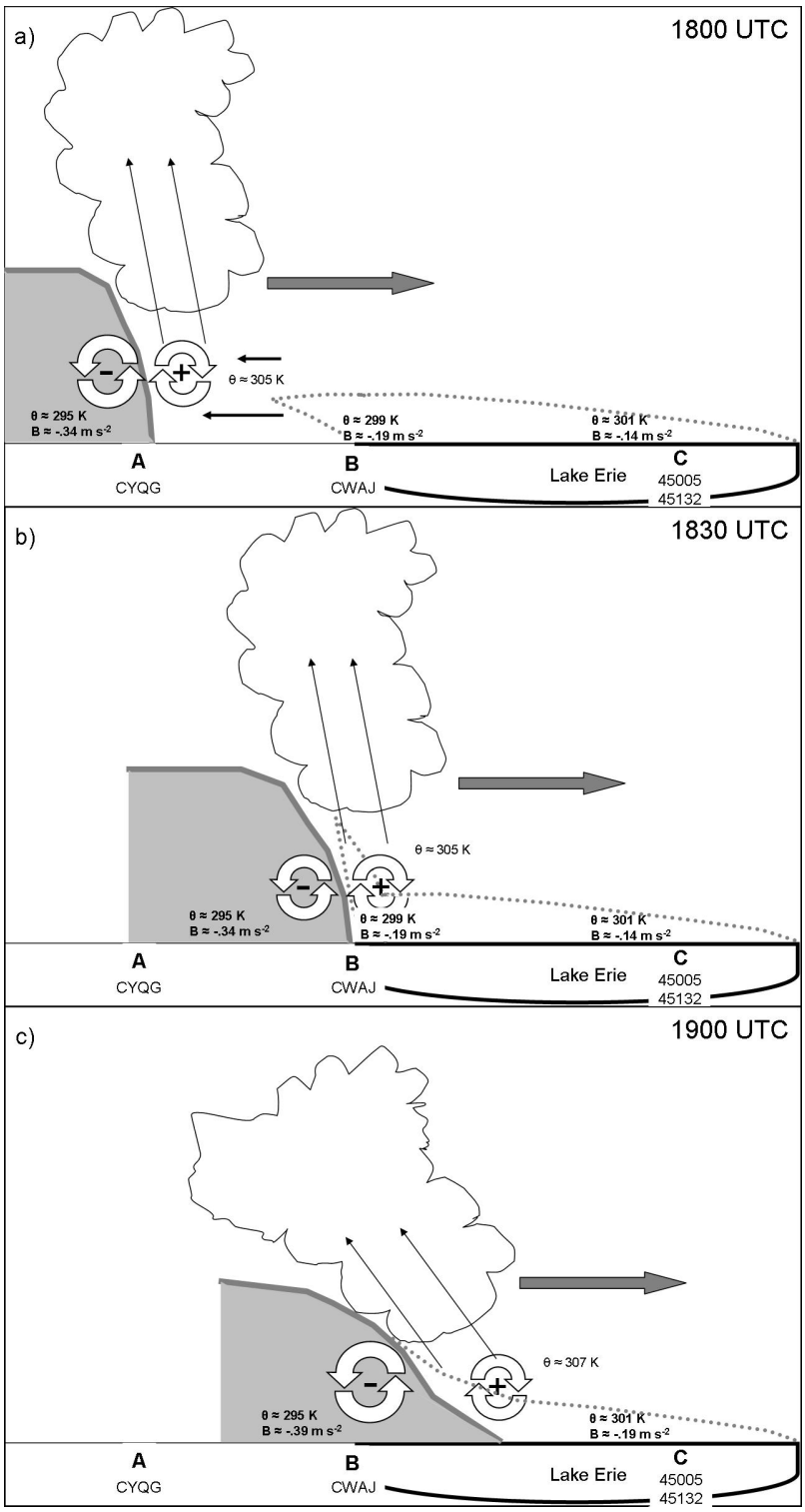

Figure 23) Conceptual diagrams (not to scale) of squall line/MBL interaction at 1800 UTC (a), 1830 UTC (b) and 1900 UTC (c). Cold pool is shaded dark gray, storm motion shown by gray arrow. θ and buoyancy (B) values determined from surface observations at the locations indicated, values at point C over Lake Erie are average values from buoys 45005 and 45132. Ambient temperature was determined from 4 locations as noted in Chapter 4.3. Location of conceptual diagrams denoted by dashed line in Figure 17.

Storm Movement (Figure 23)	MBL Depth	MBL Vorticity Tendency	Surface-based CIN	Surface Friction	Cold Pool Buoyancy Gradient	Intensity (Max dBZ)
A to B	Increased	Positive	Increased	No change	Decreased	Increased
B to C	Decreased	Negative	Decreased	Decreased	Increased	Decreased

Table 5) Showing the change in factors affecting squall line structure and intensity, and resulting predicted change in maximum intensity as the squall line moved across southern Ontario (Point A to B in Figure 23) and across Lake Erie (Point B to C in Figure 23)